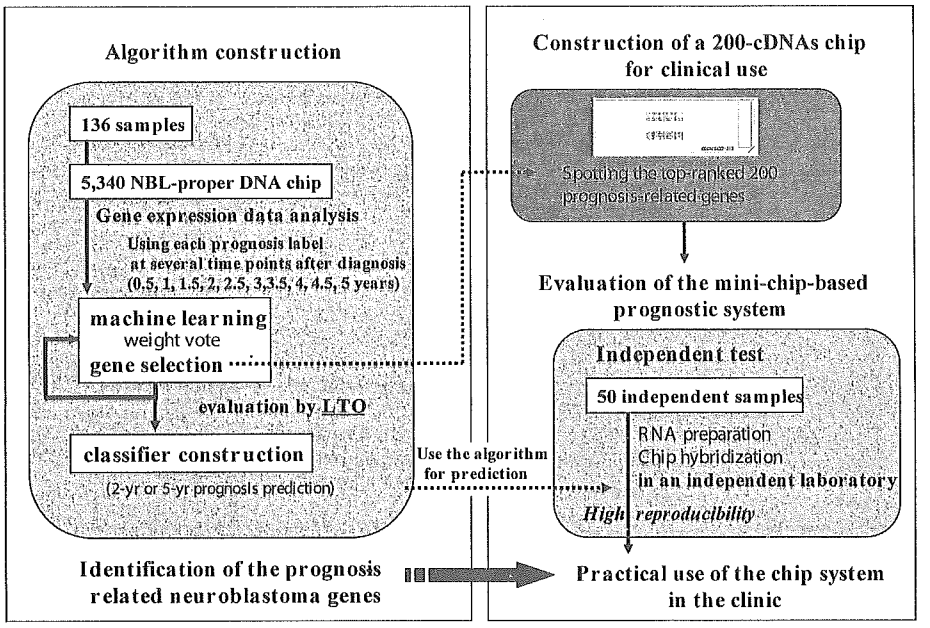

Figure 1. Schematic diagram of this study

ing a nonlinear transformation from weighted vote values to the survival rates, the transformation outputs the reliability of each sample's outcome prediction as a probabilistic output, posterior probability. We suppose each posterior probability, a real number between 0 and 1, corresponds to the expected 5 year survival rate. The right upper panel of Figure 2 shows the predictions for the 136 samples as posterior probabilities. Most of the samples alive at 5 years after diagnosis (blue mark) are found to have posterior values near 1, while most of the dead samples (red mark) have those near 0. It is known that it is difficult to predict the prognosis of neuroblastoma patients of the intermediate risk group (the type II subset: stage 3 or 4, without amplification of *MYCN*), denoted by green area. The posterior values are likely to take intermediate values near 0.5; however, their binarization after being separated by threshold 0.5 shows good accordance with the actual outcome. Frequencies of posterior values for alive and dead samples are shown in the right middle panel. The rate of alive samples among the whole samples, which denotes the actual survival rate, is plotted against each posterior value in the right bottom panel in Figure 2; this panel shows the good correspondence between the posterior value and the survival rate.

Probabilistic outputs are considered to be advantageously useful as compared with conventional binary outputs when used in making a clinical assessment and may be considered identical to them if establishing an appropriate threshold value. The real-valued posterior can be used for categorization into arbitrary number of groups. For example, dividing the posterior values into three by setting thresholds 0.3 and 0.7, we obtain three groups whose survival curves are significantly different from each other; this tertiary categorization provides another definition of intermediate risk group based only on expression patterns (Figure S4).

Comparing the survival curves

Figure 3A shows survival curves for favorable and unfavorable patients predicted by the classifier with a binary threshold (0.5). The 5 year survival rate for the former (n = 98) was as good as 94%, while that for the latter (n = 38) was as poor as 33% ($p < 10^{-5}$). When 70 sporadic neuroblastomas were evaluated after excluding the tumors found by mass screening, the 5 year survival rate for the former (n = 40) was 85%, while that for the latter (n = 30) was 20% ($p < 10^{-5}$) (Figure 3B). To further evaluate the efficiency of our system, we calculated the posterior value for the intermediate subset of neuroblastoma (type II), whose prognosis is usually difficult to predict. As shown in Figure 3C, the survival curves were significantly categorized into two groups. The 5 year survival rate of patients who were predicted as favorable was 89%, while that for unfavorable patients was 36% ($p = 0.000067$). Since the age at diagnosis (≥ 1 year) is currently used as a poor prognostic factor for the type II tumors, we examined the ability of the classifier for the older patients with type II tumors. Even for such patients whose prognosis is difficult to predict, the survival rate (45%) of all 18 patients was divided solely by gene expression into the group with favorable prognosis (n = 10; 73%) and that with poor outcome (n = 8; 13%) (Figure 3D). In addition, if the intermediate risk group was further separated into stage 3 tumor group and stage 4 tumor group, the posterior value was significantly related to the survival, especially for stage 3 tumors (Figure S5). These results suggest that the posterior value obtained by our statistical analysis highly efficaciously allows the classification of patient outcomes, even when the tumor is of the intermediate type.

We further compared our results to existing prognosis markers in Table 1 and found that the supervised microarray analysis showed the best sensitivity-specificity balance among the prognostic factors for predicting the outcome of neuroblastoma. When the classifier is combined with the age at diagnosis, the disease stage (stage 1, 2, or 4s versus stage 3 or 4) and the *MYCN* amplification, accuracy, sensitivity, and specificity increased up to 95.8%, 93.3%, and 97.0%, respectively. Although the currently used markers (age, stage, and *MYCN*)

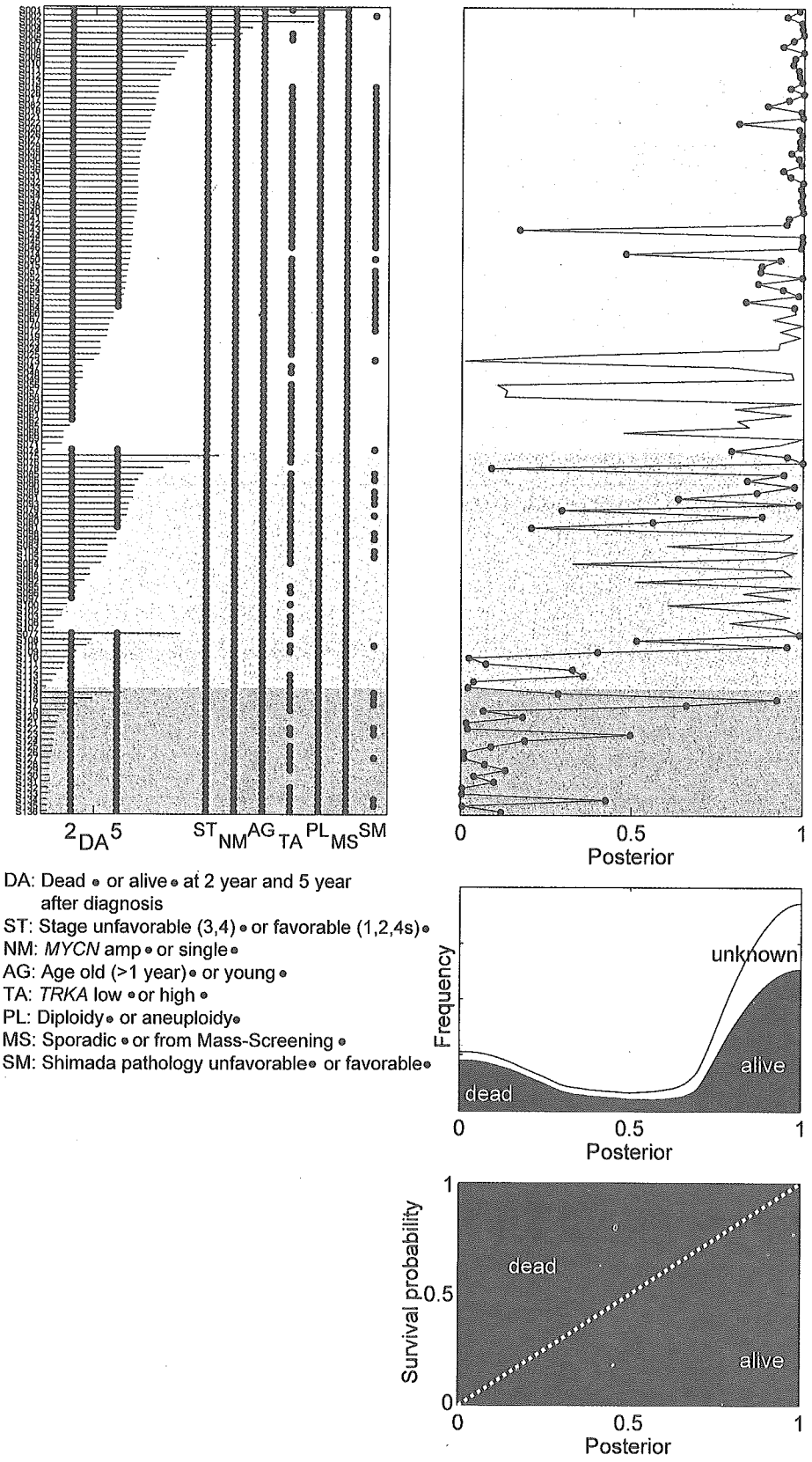

Figure 2. Posterior probability of survival at 5 years

Posterior probability of survival at 5 years for 136 training data samples, output by the leave two out (LTO) crossvalidation without any information leakage. Left panel: Neuroblastoma samples. A red or blue horizontal line denotes survival period after diagnosis for a dead or alive patient, respectively. Red and blue marks denote various clinical properties of patients; see text below the panel for detailed explanation. Background colors show groups determined by stage and *MYCN* amplification status: red, type III, with *MYCN* amplification; green, type II, with single copy of *MYCN* at unfavorable stage (3 or 4); and blue, type I, with single copy of *MYCN* and at favorable stage (1, 2, or 4s). Right upper panel: The LTO crossvalidated prediction (posterior) for each patient; a red or a blue mark denotes that the patient is dead or alive at 5 years, respectively. Right middle panel: Cumulative smooth histogram of posterior probabilities for patients of dead (red), alive (blue), and unknown (white) at 5 years after diagnosis. Right lower panel: The horizontal and vertical axes denote the posterior and the empirical probability of 5 year survival, i.e., the ratio of the smooth histogram values between dead and alive patients, shown in the middle panel, respectively. Because the border between dead and alive samples is close to the white broken line (x = y), the posterior can be regarded as a 5 year survival chance rate.

Table 1. Accuracy of each marker for prognosis prediction (5 years after diagnosis)

	Whole cases				Sporadic cases		Intermediate and old age[a]	
	n	accuracy	sensitivity	specificity	n	accuracy	n	accuracy
Microarray classifier	136	89%	87%	89%	56	82%	14	86%
Age (less than 1 year old)	136	81%	83%	80%	56	71%	14	64%
Stages (1, 2, and 4s)	136	83%	97%	77%	56	84%	14	64%
Shimada classification (unfavorable)	62	87%	78%	89%	25	72%	(n < 10)	—
Hyperdiploidy (aneuploidy)	62	72%	67%	73%	27	56%	(n < 10)	—
MYCN amplification	136	89%	67%	99%	56	80%	14	36%
Microarray + age + stages + MYCN*	136	96%	93%	97%	56	93%	14	86%

Sensitivity/specificity is the rate of unfavorably/favorably predicted samples, i.e., LTO posterior <0.5/>0.5, among actually unfavorable/favorable samples. Microarray classifier, supervised classification based on the microarray data. *By this classifier, all patients with the *MYCN* amplification are predicted as unfavorable, and all patients with a single copy of *MYCN* and at stage 1, 2, or 4s are predicted as favorable. In the remaining intermediate samples (with a single copy of *MYCN* and at stage 3 or 4), the patients with age <1 year are predicted as favorable, and the microarray predictions are applied for those with age >1 year.
[a] Age at diagnosis >1 year.

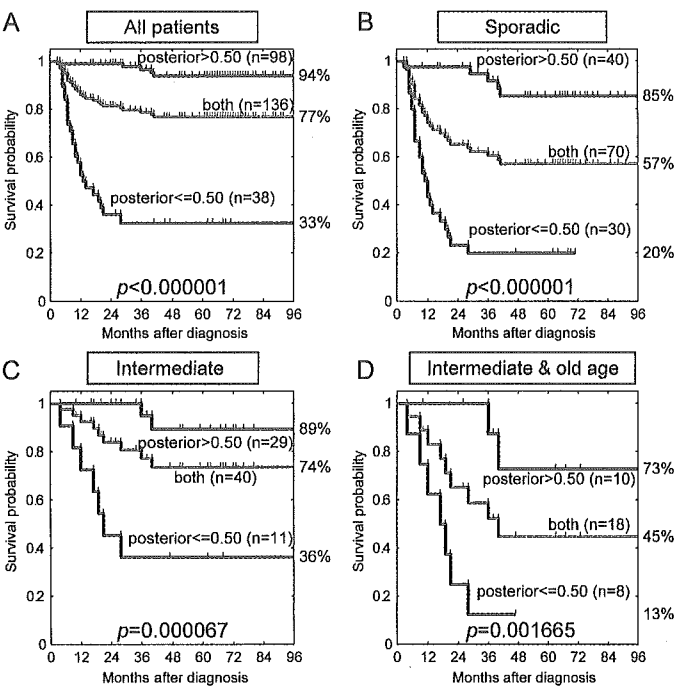

Figure 3. Disease-free survival of patients who were stratified based on the gene expression patterns

For each of the four figures, whole objective patients (green) are divided into favorable (blue) or unfavorable (red) based on the posterior values with threshold 0.5, which are calculated from gene expression patterns, and statistical features of their survival times are denoted by the Kaplan-Meier survival curves. The differences of the survival curves between the favorable (blue) and unfavorable (red) groups are evaluated by p values of the log rank test.

A and B: Survival analysis of whole and sporadic patients, respectively, divided by the supervised classifier based on microarray data.

C and D: Survival analysis of patients in the intermediate risk group with different definitions, divided by the supervised classifier. The intermediate risk group shown in (C) is defined as *MYCN* single and stage 3 or 4 (type II), and that in (D) is defined as *MYCN* single, stage 3 or 4, and older than 1 year of age.

also showed good potential to predict generally but less than the microarray, these exhibited only 64% accuracy of prediction for the type II tumors with $\geq$1 year of age (Table 1). Together with the results of survival analysis, the microarray classifier is revealed to be a powerful predictor to classify such group of neuroblastomas (86% accuracy; Table 1).

Practical application of 200 cDNAs microarray and independent test

For the practical use in the clinic, a cDNA microarray system that contains cDNA spots of a relatively small number and hence is easy to treat is expected. According to our gene selection based on the pairwise *F* score, the numbers of genes that were appropriate for the 5 year and 2 year prognosis prediction for all available samples were 10 and 70, respectively. In order for the system to reserve the applicability to short-term and long-term outcome prediction simultaneously, we selected 200 top-ranked genes according to the pairwise *F* scores in the 2 year prediction, because the 2 year prediction required larger variety of genes, and then made a smaller cDNA microarray system carrying the 200 genes. The newly designed microarray system (the mini-chip system) was evaluated by being hybridized with 5 μg total RNA obtained from 50 independent test samples. To preserve the independence of experimental procedure, these RNAs were prepared and hybridized in a different laboratory from the original experiments of 136 samples with the 5340 genes system (see Experimental Procedures). Although the weight values in the weighted voting classifier were determined by the 5340 genes system without any information leakage from the 50 independent samples, the result was as good as that obtained by the 5340 cDNA microarray analysis (90% [45/50] for 2 year, and 87.8% [43/50] for 5 year prognosis prediction; Figure 4B). This test validated not only the prediction robustness of our classifier constructed by the 5340 genes system, but also the construction procedure of the mini-chip system according to our gene selection based on pairwise *F* scores. When we reconstructed another supervised classifier by applying the LTO analysis to the 50 samples measured by the mini-chip system, the accuracy of the 5 year prediction was 91.8% (45/49) (Figure 4C). These results suggest

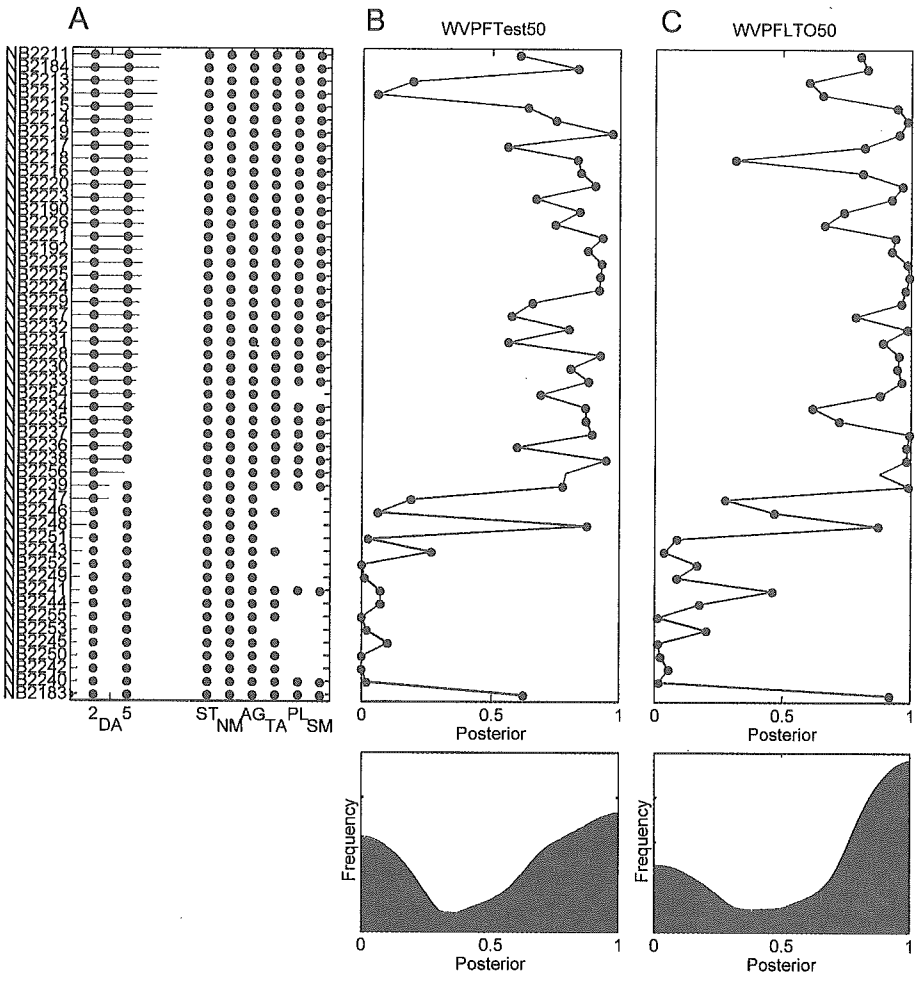

Figure 4. Posterior probability of survival at 5 years for test samples

Posterior probability of survival at 5 years for 50 independent test samples measured by newly developed 200 genes chip (the mini-chip system). Left panel: Neuroblastoma samples; see also Figure 2 legend. Center panel: Prediction results when the supervised classifier constructed from 96 training samples is applied to the 50 independent samples (independent test for the classifier's reproducibility). Right panel: LTO crossvalidation analysis using the new 50 samples (test for the procedure's reproducibility). Both tests do not introduce any information leakage. Lower panels: Smooth histograms of posterior probabilities for dead (red) and alive (blue) patients.

three things. (1) The supervised classifier obtained by the statistical analysis by the 5340 genes system is reproducible even if it is applied to the data measured by the reduced 200 genes system. Note that the 50 samples were completely new data for the classifier in this case. (2) Our procedure to construct a supervised classifier according to the LTO analysis is also reproducible, because the same procedure was successful in making another classifier with a high prediction accuracy when applied to the data taken by the mini-chip system. (3) A simple, low-cost microarray system, the mini-chip system, is highly feasible for predicting the prognosis of neuroblastoma.

Genes selected for prognosis prediction

To assess the relationship between the clinically defined subsets of neuroblastoma and the expression of 70 genes that were selected as top scored with 2 year prognosis according to the pairwise *F* score, we conducted an unsupervised clustering analysis (Figure 5). As expected, part of the type II (intermediate) tumors of patients with a poor prognosis showed an expression pattern that was similar to that of the type III (unfavorable) tumors, and many of them died. On the other hand, expression profiles of the remaining type II tumors seemed to be heterogeneous similarly to those of the type I (favorable) tumors with a good outcome. Most of the tumors with highly expressed *TrkA* and hyperdiploidy, as well as tumors detected by mass screening, were included in the latter group. Table 2 shows a list of 41 genes that corresponded to the 70 top-scored genes and their p and q values (Storey and Tibshirani, 2003) in the log rank test, since we found that several genes were duplicated in the selected 70 genes. Based on the above clustering, these genes were categorized into two groups (group F and group UF; the gene groups strongly correlated with favorable and unfavorable prognosis, respectively) (Figure 5 and Table 2).

The genes in group F tended to show high levels of expression in the type I tumors, while those in group UF were highly expressed in the type III tumors. The former contained genes that were related to neuronal differentiation (*tubulin* α, *peripherin*, *neuromodulin* [*GAP43*], and *HMP19*) and genes that were related to catecholamine metabolism (*dopa decarboxylase* [*DDC*], *dopamine* β-*hydroxylase* [*DBH*], and *tyrosine hydroxylase* [*TH*]). On the other hand, the latter involved many members of genes that are related to protein synthesis (ribosomal protein genes such as *RPL18A*, *RPLP0*, *RPL5*, *RPL4*, and *RPL7A* as well as translation initiation and elongation factor genes *EEF1G* and *EIF3S5*) and genes that are related to me-

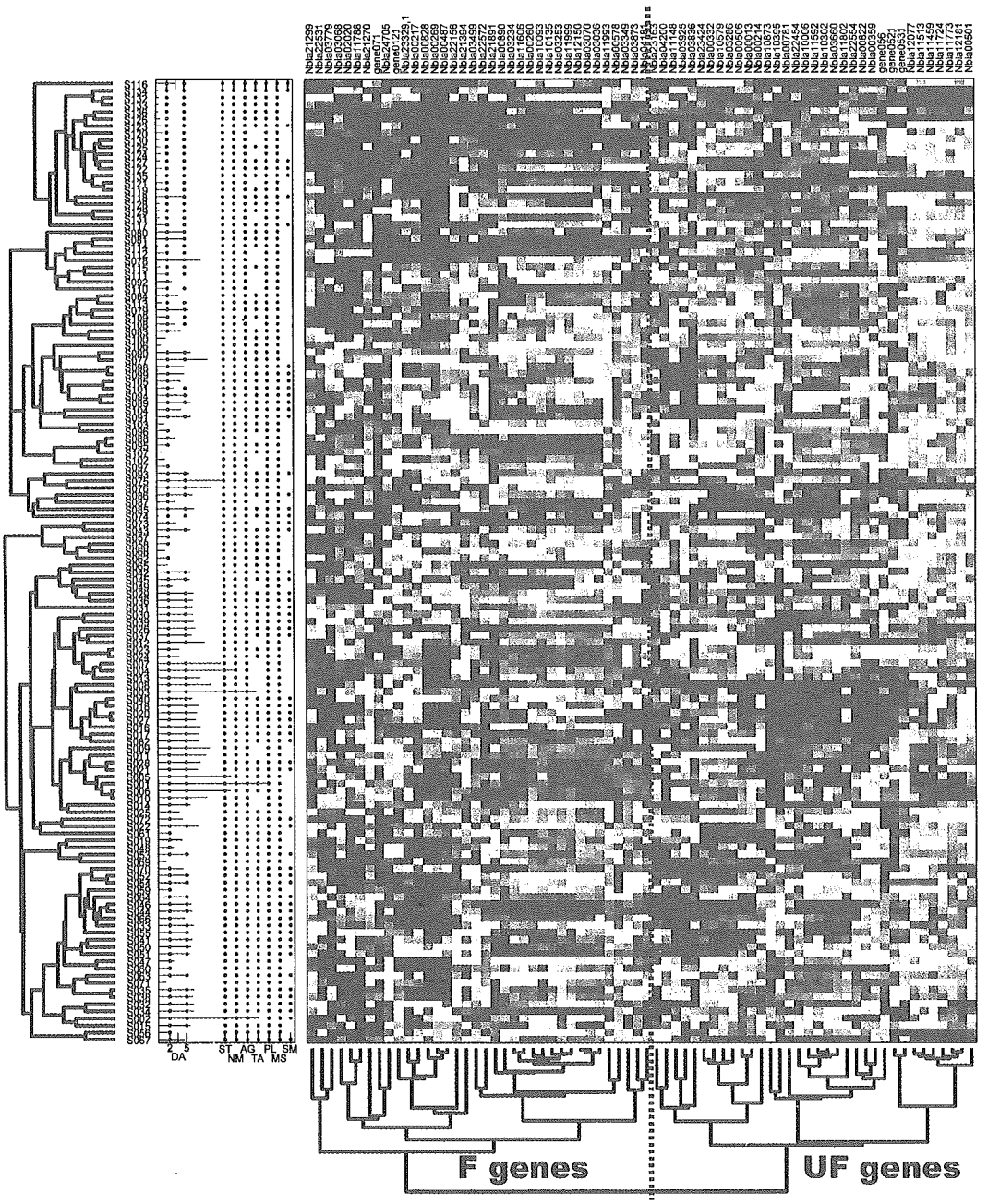

Figure 5. Expression profiles of 70 genes selected for predicting neuroblastoma prognosis at 2 years

Note that 10 genes for predicting prognosis at 5 years are also included in the 70 genes. The left and lower trees depict hierarchical clustering of the 136 neuroblastoma samples and the 70 genes selected in the present study, respectively. In the left tree, blue, green, and red colors denote "*MYCN* single and stage 1, 2 or 4s tumor" (type I, favorable), "*MYCN* single and stage 3, 4 tumor" (type II, intermediate), and "*MYCN* amplified tumor" (type III, unfavorable), respectively. The blue and red colors in the expression matrix show the high and low expression, respectively. A gene showing high expression level likely for unfavorable samples belongs to the group "UF" (red subtree in the lower tree), while one showing high expression likely for favorable samples belongs to the group "F" (blue subtree in the lower tree).

tabolism (*enolase 1* [*ENO1*] and *transketolase* [*TKT*]). The top 10 genes selected for the 5 year outcome prediction were *RPL18A*, *ENO1*, *EEF1G*, *TUBA3*, *GNB2L1*, *ARHGEF7*, *GCC2*, *DDX1* (duplicated), and *PRPH*. The *MYCN* gene was also a member of 70 genes (group UF) as expected; however, it was outside of the top 10 genes for the 5 year label. Instead, *DDX1*, which is frequently coamplified with *MYCN* on chromosome 2p24, was a member of the top 10 genes (UF group) for both of the 2 year and 5 year labels. Confirmation of the differential expression of the selected genes was further conducted by

Table 2. Top-ranked genes used for prediction of 2 year and 5 year prognosis of neuroblastoma

	Spot name	Accession number	Gene code	Chromosome map	Pattern	Log rank p	q value
F group							
	Nbla11606	NM_006009	*TUBA3*	12q13.12	F > UF	0	0.000674
	Nbla00890	NM_003899	*ARHGEF7*	13q34	F > UF	0.000001	0.000743
	Nbla00260	NM_006082	*K-ALPHA-1*	12q13.12	F > UF	0.000003	0.000926
	Nbla21891	U87309	*VPS41*	7p14.1	F > UF	0.000006	0.001096
	Nbla03873	NM_006054	*RTN3*	11q13.1	F > UF	0.00001	0.001282
	Nbla11788	NM_006262	*PRPH*	12q13.12	F > UF	0.000017	0.001522
	Nbla10093	NM_000183	*HADHB*	2p23.3	F > UF	0.000018	0.001541
	Nbla22572	NM_000790	*DDC*	7p12.2	F > UF	0.000035	0.00213
	Nbla21270	NM_001915	*CYB561*	17q23.3	F > UF	0.00016	0.00495
	gene071	NM_000360	*TH*	11p15.5	F > UF	0.000787	0.012173
	Nbla03499	NM_002074	*GNB1*	1p36.33	F > UF	0.000795	0.012237
	Nbla04181	AK55112	*AK55112*	5q13.2	F > UF	0.001425	0.017462
	Nbla00487	AB075512	*C6orf134*	6p21.33	F > UF	0.002751	0.025273
	Nbla00269	NM_000787	*DBH*	9q34.2	F > UF	0.00362	0.030407
	Nbla22531	NM_002045	*GAP43*	3q13.31	F > UF	0.004394	0.034175
	Nbla22156	NM_014944	*CLSTN1*	1p36.22	F > UF	0.005233	0.038274
	Nbla00578	NM_006818	*AF1Q*	1q21.3	F > UF	0.009397	0.05354
	Nbla00217	NM_032638	*GATA2*	3q21.3	F > UF	0.010245	0.056301
	Nbla21394	NM_000743	*CHRNA3*	15q25.1	F > UF	0.072464	0.162629
	Nbla11993	NM_015980	*HMP19*	5q35.2	F > UF	0.204274	0.282486
UF group							
	Nbla00214	NM_000980	*RPL18A*	19p13.11	F < UF	0.000002	0.001107
	Nbla00013	NM_006098	*GNB2L1*	5q35.3	F < UF	0.000006	0.001051
	Nbla11459	NM_004939	*DDX1*	2p24.3	F < UF	0.000024	0.001795
	Nbla11148	NM_001002	*RPLP0*	12q24.23	F < UF	0.000049	0.002549
	Nbla00332	NM_001404	*EEF1G*	11q12.3	F < UF	0.000055	0.002696
	Nbla10395	NM_002593	*PCOLCE*	7q22.1	F < UF	0.000164	0.005009
	Nbla03286	NM_020198	*GK001*	17q23.3	F < UF	0.000175	0.005204
	Nbla23163	NM_003754	*EIF3S5*	11p15.4	F < UF	0.000341	0.007105
	Nbla10579	NM_181453	*GCC2*	2q12.3	F < UF	0.000962	0.01407
	Nbla00359	NM_003550	*MAD1L1*	7p22.3	F < UF	0.00112	0.01525
	gene052-1	NM_005378	*MYCN*	2p24.3	F < UF	0.001253	0.016367
	Nbla03925	NM_002295	*LAMR1*	3p22.2	F < UF	0.001773	0.01931
	Nbla23424	NM_001404	*EEF1G*	11q12.3	F < UF	0.003579	0.030326
	Nbla22554	NM_000687	*AHCY*	20q11.22	F < UF	0.003946	0.032409
	gene056	NM_000546	*TP53*	17p13.1	F < UF	0.004087	0.032829
	Nbla10873	NM_005762	*TRIM28*	19q13.43	F < UF	0.004984	0.037476
	Nbla00501	NM_000969	*RPL5*	1p22.1	F < UF	0.005786	0.04012
	Nbla10302	NM_001428	*ENO1*	1p36.23	F < UF	0.007702	0.048179
	Nbla04200	NM_000968	*RPL4*	15q22.31	F < UF	0.04097	0.120453
	Nbla03836	NM_000972	*RPL7A*	9q34.2	F < UF	0.048031	0.132345
	Nbla00781	NM_001064	*TKT*	3p21.1	F < UF	0.048075	0.132342

Although 70 clones were selected as important genes for the supervised classifier, duplicated and multiplicated clones are omitted in this table. The 41 genes are classified into two groups, "F > UF" and "F < UF," when the expression in favorable samples is higher than that in unfavorable samples, and vice versa, respectively. In each group, genes are sorted by log rank p values. The log rank p value for each gene was calculated by comparing survival curves of two patient groups, in which the expression of the gene is higher and lower, respectively, than the median over the samples. A "q value" of a gene denotes the estimated false discovery rate among the genes whose p value is the same or smaller than that of the gene, and is a p-like value while incorporating multiplicity of the statistical test.

using representative 16 favorable and 16 unfavorable tumor samples that were independent of the 136 samples used in the present analysis, by semiquantitative RT-PCR (Figure S6; refer also to Ohira et al., 2003a). We also conducted immunohistochemical analysis for peripherin antibody using tissue sections prepared from primary neuroblastoma with favorable and unfavorable histology, since peripherin gene is a member of the top 10 genes for both 2 year and 5 year outcome prediction (Table 2). Peripherin protein was positively detected in the cytoplasm of neuroblastic cells as well as neuritis in all three favorable histology tumors (Figure S7, FH&NA). Two unfavorable histology tumors with poorly differentiated subtype, regardless of *MYCN* status, showed sporadic staining (less than 20% of the favorable histology tumor) for peripherin protein in neurites. Peripherin was completely negative in the unfavorable histology tumor of undifferentiated subtype (Figure S7, UF&NA). These results indicate the reliability of our gene selection. In the log rank test, p values of 18 of 20 genes in group F and of all 21 genes in group UF were less than 0.05 (Table 2), indicating that these 39 genes can be independent prognostic factors for primary neuroblastomas.

Discussion

Our study has disclosed the molecular signature of neuroblastoma that predicts patient outcomes by using RNA ob-

tained from 136 primary neuroblastomas. The highly reliable statistical analysis by using a neuroblastoma proper cDNA microarray harboring 5340 genes based on an electrically controlled ceramics-based ink-jet method led us to design a cDNA microarray system harboring 200 genes, which is applicable to short-term (2 year) and long-term (5 year) prognosis predictions for neuroblastoma.

Our study demonstrated that the supervised classifier produced by the 5340 genes system provided a high accuracy (88.5%) for the 5 year outcome prediction, with a good balance between sensitivity (86.7%) and specificity (89.4%). Although age at diagnosis, disease stage, *MYCN* amplification, and patients found by mass screening have been useful prognostic markers currently used at the bedside, most of them have either high sensitivity or high specificity (Table 1). The microarray analysis showed the best sensitivity-specificity balance among the prognostic factors for predicting the outcome of neuroblastoma. When the classifier is combined with the age at diagnosis, the disease stage (stage 1, 2, or 4s versus stage 3 or 4) and the *MYCN* amplification, accuracy, sensitivity, and specificity increased up to 95.8%, 93.3%, and 97.0%, respectively. Furthermore, the intermediate subset of neuroblastomas (type II), for which a long-term prognosis is usually difficult to make, was also categorized by microarray analysis into groups of patients with a favorable prognosis and those with an unfavorable prognosis. These successful results led us to produce a more practical tool at the bedside, the mini-chip system, whose accuracy, sensitivity, and specificity were 87.8%, 76.5%, and 93.8%, respectively, when the classifier constructed by the 5340 genes system was applied to 50 independent samples measured by the mini-chip system, and were 91.8%, 82.4% and 96.9%, respectively, when another classifier was constructed by applying the LTO procedure to the same data (Figure 4).

It is well recognized now that gene expression analyses for cancer prognosis prediction should pay close attention to the reproducibility of obtained results. A complete crossvalidation analysis without introducing any information leakage and an independent test using new samples are necessary. Although the determination of the appropriate number of genes used in supervised classifiers should be included in the validation procedure, it has often been ignored in most microarray studies. van 't Veer et al. (2002) applied the supervised classification to the breast cancer gene signature, which is predictive of a short interval to distant metastases in 78 patients who were initially devoid of local lymph node metastasis. Although their crossvalidation analysis without the validation of the number of genes correctly predicted the actual outcome of disease for 63 of 78 patients (80.7%), the accuracy was worse when a complete validation was applied (73.1%). This difference suggests that even small information leakage may lead to overestimation of the accuracy. Beer et al. (2002) applied the supervised classification to the outcome prediction of lung adenocarcinoma. Their statistical analysis was complete without any information leakage. They did not report the prediction accuracy, but we estimated the accuracy to be about 70% from the data in their paper and found that the prediction by their supervised classifier was not very superior to that by existing prognosis markers. Iizuka et al. (2003) applied the supervised classification to the prediction of intrahepatic recurrence within 1 year after curative surgery for hepatocellular carcinoma patients. Although their predictor showed sufficiently high accuracy in an independent test with 27 samples, their crossvalidation procedure excluded the validation of the determination process of the number of optimum genes (steps 5 and 6 in their algorithm). The high crossvalidation accuracy of 100% may be an overestimation due to the information leakage.

According to the recent study that evaluated statistical methodologies used by microarray studies published between 1995 and April 2003, the three papers above were the only ones that reported both fairly sound crossvalidation analyses and independent tests (Ntzani and Ioannidis, 2003). Our LTO procedure includes the validation process of the number of genes used in the classifier and hence is a complete crossvalidation process. In addition, the obtained classifier was applied to the 50 independent samples that were measured by the reduced 200 genes system. This is a stronger test than usual independent tests but is important for the development of a practical system at the bedside. In addition, our LTO analysis achieved an almost unbiased estimation of the accuracy. Our crossvalidation analysis using the LTO procedure, the independent test of the classifier, and the validation of the procedure itself within a new experimental environment using the mini-chip system exhibited one of the most conservative and reliable statistical methodologies. In addition, our gene selection procedure according to the pairwise F score tries to extract correlation structures among genes, based on an idea similar to the exhaustive optimization method used in Iizuka et al. (2003), is beneficial in enhancing the applicability of the mini-chip system to various prediction problems, namely, short-term and long-term outcome predictions.

In addition to high accuracy, another advantage of our method is to provide a type of predictive information beyond the conventional binary prediction like favorable and unfavorable, which is ambiguous. The probabilistic output based on the hypothetical distribution obtained by the LTO analysis, the posterior probability, was found to show good accordance with actual survival rate (right bottom panel in Figure 2); this enables us to make a simple interpretation of the output: a patient with a posterior value of 0.8 has 80% chance for the 5 year survival, for example. Moreover, by calculating posterior probabilities for various future time points, a survival chance curve for each patient can be depicted (Figure 6). Although the follow-up period of patient "S057" is 2 years, and the patient is alive at this time, the individual survival chance curve says that his/her survival chance estimated from the gene expression pattern at diagnosis will get smaller than 50% at about 3 years after diagnosis. Such an individual survival chance curve can be used in choosing a suitable therapeutic protocol.

Another advantage of our method is that the probabilistic output is very stable in the presence of noise. Even when an artificial noise, whose variance is as large as the estimated noise variance of microarray, was added to expression profile data, prognosis prediction did not degrade very much (Figure S8). This robustness was confirmed when the noise variance went up to 1.0, which was sufficiently greater than the actual reproduction noise level of 0.4 (Figures S1A–S1C).

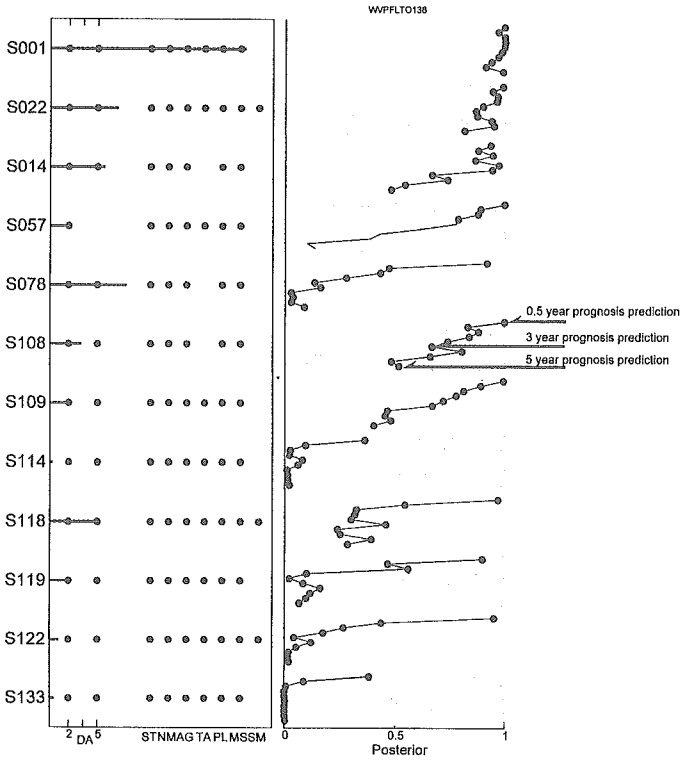

Figure 6. Individual survival chance analysis based on posterior probabilities

LTO estimation of survival probabilities at 0.5, 1.0, 1.5, ..., 5.0 years after diagnosis for 12 typical patients. Left panel: Information of patients (see caption of Figure 2). Right panel: Estimated posterior probabilities at 0.5, 1.0, 1.5, ..., 5.0 years after diagnosis, which predict the time course of patient's survival chance. A blue or a red mark denotes that the patient is alive or dead at that time after diagnosis, respectively. For example, the patient "S108," who died at 40 months, is predicted as 100% alive at 0.5 year and 52% alive at 5 year, solely from the microarray analysis at the diagnosis

The high outcome predictability of our system is attributable to multiple reasons. The quality of tumor samples is high because (1) an appropriate system was established for our neuroblastoma tissue bank, and (2) handling of tumor tissues is rather uniform at each hospital, in which informed consent was obtained. An array, produced by a new apparatus equipped with a piezo microceramic pump, generates highly reproducible signals. The noncontact spotting method makes the spot shape almost a perfect circle. Consequently, the spot excels in signal uniformity. We did not conduct microdissection of the 136 tumor samples, because the stromal components of the tumor, e.g., Schwannian cells, are already known to be very important to characterize its biology (Ambros and Ambros, 1995; Ambros and Ambros, 2000). Therefore, a good combination or selection of these procedures may have provided high outcome predictability. In addition, the high predictability was reliably confirmed by the complete crossvalidation analysis and the independent test. The probabilistic output based on the LTO analysis can provide a new type of information that will improve the therapeutic decision at the bedside. In addition, the probabilistic output is highly robust against noises that may be involved in test samples (described above); this can be the major reason for the high prediction accuracy when the classifier constructed by the 5340 genes system was applied to the data taken by the mini-chip system.

The impact of the selected genes is strong. The genes with the highest score in F group genes (F > UF) were *tubulin* α members (*TUBA3* and *K-ALPHA-1*, which corresponds to *TUBA1*), which have never been reported to be prognostic factors in neuroblastoma. Their prognostic significance has also been confirmed by RT-PCR in primary tumors (data not shown). The high expression of *TUBA1* in neuronal cells is associated with axonal outgrowth during development as well as with axonal degeneration after axotomy in adult animals (Knoops and Octave, 1997). The expression of *TUBA3* has been reported to be restricted to adherent, morphologically differentiated neuronal and glial cells (Hall and Cowan, 1985). We have also found that high expression of *tubulin tyrosine ligase* and enhanced tubulin tyrosination/detyrosination cycle are associated with neuronal differentiation in neuroblastomas with favorable prognosis (Kato et al., 2004). Thus, high mRNA expression of *TUBA* genes in favorable neuroblastoma may reflect differentiated status of tumors. ARHGEF7, Rho guanine nucleotide exchange factor 7, activates Rho proteins by exchanging bound GDP for GTP and can induce membrane ruffling. In our previous paper, we found that many family members of such G protein-related genes are highly expressed in favorable neuroblastomas compared to unfavorable ones (Ohira et al., 2003a). This may also imply a neuronal maturity nature of favorable tumors. Peripherin, a type III intermediate filament protein, was initially found as a cytoskeletal protein in the peripheral nervous system and in cultured cells of neuronal origin. This protein is known to be a marker of terminal neuronal differentiation; however, its functional role in neuroblastoma has been elusive. The previous evidence indicates that peripherin is transcriptionally upregulated by treatment with NGF, an important neurotrophin in neuroblastoma, and that the protein product is directly phosphorylated by NGF receptor, TrkA (Aletta et al., 1989). Thus, peripherin may play an important role as one of the signal transduction components involved in elaboration and maintenance of neuronal differentiation. In the UF gene group, many ribosomal protein-related genes are selected. *GNB2L1*, a receptor for activated C-kinase *RACK1*, is implicated in linking between *PKC* signaling and ribosome activation (Ceci et al., 2003). The *DDX1* gene, which is frequently coamplified with the *MYCN* gene in advanced neuroblastomas (Godbout and Squire, 1993; Noguchi et al., 1996), is also a member of this group. Its protein product is a putative RNA helicase and is implicated in a number of cellular processes involving alteration of RNA secondary structure such as translation initiation, nuclear and mitochondrial splicing, and ribosome and spliceosome assembly. *DDX1* is ranked at a higher score than the *MYCN* gene, which is concordant with the previous reports describing that *MYCN* mRNA expression is a weaker prognostic marker than its genomic amplification (Slavc et al., 1990). Another important prognostic factor, *TrkA*, is not included in the top 70 genes but in the 90 (in the top 20 genes when the 5 year label was used) (data not shown), probably due to its relatively low levels of mRNA expression as compared with those of other genes. The prognos-

tic effect of *TrkA* expression may be compensated by other genes which are affected or regulated by *TrkA* intracellular signaling. Similarly, *MYCN*-regulated genes such as ribosomal genes, translation initiation and elongation factors, and laminin receptor may compensate the effect of *MYCN* gene expression in aggressive tumors. It is intriguing that high mRNA expression of *p53* gene is also strongly related to unfavorable outcome. Although *p53* mutation is rare in primary neuroblastomas, and its gene product frequently accumulated in cytoplasm, an unknown mechanism that upregulates *p53* expression in aggressive tumors may exist.

Our results showed that the decision by majority by the genes selected based on microarray data alone can be a prognostic indicator comparative to the existing prognostic markers, and that the addition of the microarray data to the prognosis markers improved the outcome prediction (Table 1). The outcomes of patients belonging to the intermediate subset, whose prognosis prediction had been very difficult by existing prognosis markers, were effectively separated into favorable group and unfavorable group ($p < 10^{-4}$). The posterior value will help the decision of therapeutic modalities, and outcome prediction based on the posterior value is extremely robust against a possible noise. In addition, our practical, low-cost microarray carrying only 200 genes should make its clinical use possible. Our further validation by hybridizing RNA obtained from 50 fresh neuroblastomas on the 200 cDNAs microarray in a completely independent laboratory indicated that our prediction system is consistent and feasible. Therefore, the application of a highly qualified cDNA microarray at the bedside may bring tailored medicine that allows better treatment of neuroblastoma patients.

Experimental procedures

Patients and tumor specimens

Fresh, frozen tumor tissues were sent to the Division of Biochemistry, Chiba Cancer Center Research Institute, from a number of hospitals in Japan (1996–2002). Informed consent was obtained at each institution or hospital. We randomly selected tumor samples from this neuroblastoma tissue bank and then successfully conducted hybridization in 136 neuroblastomas consisting of 41 stage 1 tumors, 22 stage 2 tumors, 33 stage 3 tumors, 28 stage 4 tumors, and 12 stage 4s tumors. Among the 136 fresh neuroblastomas, seventeen tumors were obtained at the delayed primary surgery after giving chemotherapy, but the other 119 tumors were resected by biopsy or surgery without giving any therapy. After surgery, patients were treated according to the previously described common protocols (Kaneko et al., 1998). Biological information on each tumor, including *MYCN* gene copy number, *TrkA* gene expression, and DNA ploidy, was analyzed in our laboratory, as described previously (Hishiki et al., 1998). All the tumors were classified according to the International Neuroblastoma Staging System (INSS) (Brodeur et al., 1993). The stage 4s neuroblastoma shows a special pattern of clinical behaviors, and the tumor itself, as well as its widespread metastases to the skin, liver, or bone marrow, usually regresses spontaneously. For a better understanding of statistical results, we introduced Brodeur's classification of neuroblastoma subsets: type I (stages 1, 2, or 4s; a single copy of *MYCN*; blue marks in Figure 2), type II (stage 3 or 4; a single copy of *MYCN*; green marks in Figure 2), and type III (all stages; amplification of *MYCN*; red marks in Figure 2) (Brodeur and Nakagawara, 1992). Among 136 tumors that we analyzed, 66 were found by mass screening of urinary catecholamine metabolites at the age of 6 months, which has been performed nationwide in Japan from 1984 to 2004 (Sawada et al., 1984). The follow-up duration ranged between 3 and 241 months (median, 56 months; mean, 57.3 months) after diagnosis. All diagnoses of neuroblastoma were confirmed by the histological assessment of a surgically resected tumor specimen at each hospital. Shimada's classification (Shimada et al., 1984) was performed in 62 out of 136 cases. The macroscopic necroses in the tumor were excluded from the tissue sampling for molecular analysis. We used for the microarray analysis only the tumor samples whose adjacent tissues contained more than 70% tumor cells in the thin sections stained with hematoxylin-eosin. For independent test, 50 (19 were found by mass screening and 31 were clinically found) tumors (15 of stage 1, 6 of stage 2, 9 of stage 3, 14 of stage 4, and 6 of stage 4s) were used.

Total RNA was extracted from each frozen tissue according to the AGPC method (Chomczynski and Sacchi, 1987). RNA integrity, quality, and quantity were then assessed by electrophoresis on the Agilent RNA 6000 nanochip using Agilent 2100 BioAnalyzer (Agilent Technologies, Inc.).

cDNA microarray experiments

We previously obtained approximately 5,000 genes after selecting from 10,000 clones randomly picked up from the mixture of oligo-capping cDNA libraries, which were generated from three primary neuroblastomas with a favorable outcome (stage 1; high *TrkA* expression and a single copy of *MYCN*), three tumors with a poor prognosis (stage 3 or 4; low expression of *TrkA* and amplification of *MYCN*), and a stage 4s tumor (Ohira et al., 2003a; Ohira et al., 2003b). Using these isolated genes together with 80 known cDNAs that were thought to be neuroblastoma-related genes, we first constructed a neuroblastoma proper cDNA microarray (named CCC-NB5000-Chip) carrying 5340 cDNA spots (the 5340 genes system). Insert DNAs (average size, approximately 2.5kb) were amplified by polymerase chain reaction (PCR) from these cDNA clones, purified by ethanol precipitation, and spotted onto a glass slide at a high density with an ink-jet printing tool (NGK Insulators, Ltd.).

Ten micrograms each of total RNA were labeled with the CyScribe RNA labeling kit in accordance with the manufacturer's manual (Amersham Pharmacia Biotech), followed by probe purification with the Qiagen MinElute PCR purification kit (Qiagen). We used a mixture of equal amounts of RNA from each of four neuroblastoma cell lines (NB69, NBL-S, SK-N-AS, and SH-SY5Y) as a reference. RNAs extracted from primary neuroblastoma tissues and RNAs of the reference mixture were labeled with Cy3 and Cy5 dye, respectively, and were used as probes together with yeast tRNA and polyA for suppression. Subsequent hybridization and washing were conducted as described previously (Takahashi et al., 2002; Yoshikawa et al., 2000). Hybridized microarrays were scanned using the Agilent G2505A confocal laser scanner (Agilent Technologies, Inc.), and fluorescent intensities were quantified using the GenePix Pro microarray analysis software (Axon Instruments, Inc.). The procedure of this study was approved by the Institutional Review Board of the Chiba Cancer Center.

After selecting genes strongly related to the prognosis of patients with neuroblastoma (at 2 years and at 5 years after diagnosis), we constructed a 200 cDNAs microarray on glass slides by the same procedure described above (the mini-chip system). For the independent test using 50 samples, tumor RNA preparation, probe labeling, and hybridization were conducted in a completely different laboratory from the original 136 hybridization. In this independent test, 5 μg each of total RNA were used for labeling.

Data preprocessing

To remove chip-wise biases of a microarray system, we used the LOWESS normalization (Cleveland, 1979). When the Cy3 or Cy5 strength for a clone was smaller than 3, strength was regarded as abnormally small, and the log expression ratio of the corresponding clone was treated as a missing value. The rate of such missing entries was less than 1%. After normalizing the 5340 (genes) by 136 (samples) log expression matrix and removing missing values, each missing entry was imputed to an estimated value by Bayesian principal component analysis, which was developed previously (Oba et al., 2003).

Supervised machine learning and LTO crossvalidation

The 96 samples, whose prognosis at 5 years after diagnosis had been successfully checked, were used to train a supervised classifier that predicts the 5 year prognosis of a new patient. When we considered the short-term prediction, 126 samples whose 2 year prognosis is known were used. Selection of the genes that are related to the classification is an important preprocess for reliable prediction. We omitted the genes whose standard

deviation of the log ratios for the genes obtained over 136 experiments was smaller than 0.36, so that 1000 genes remained, because the background noise level was about 0.2–0.3. After the gene screening, the genes were scored by the pairwise *F* score, which is a modification of a pairwise correlation method (Bo and Jonassen, 2002), to conduct gene ranking in an attempt not only to obtain higher discrimination accuracy by using a smaller number of genes but also to reserve the applicability to various outcome prediction by the set of selected genes (see the Supplemental Data).

We used a well-established technique in the supervised classification (prognosis prediction), that is, weighted voting with linear discriminators, where each weight value was calculated as the signal-to-noise ratio (Golub et al., 1999). In the weighted voting, only n genes with the largest pairwise *F* score were used. The number of top genes, n, strongly affects the prediction accuracy (Figure S3) as found in various microarray studies and hence should be determined such to maximize the leave one out (LOO) crossvalidation accuracy. However, a naive determination process of n may introduce information leakage, and the accuracy optimized by the LOO crossvalidation involves overestimation. To avoid such an overestimation, we consulted a LTO analysis. The LTO analysis was constituted of inner and outer loops of LOO (Figure S2A); the gene number n was optimized by the LOO crossvalidation repeating the inner loops, and the optimized classifier was evaluated by an independent test for a single sample left out at a single step in the outer loop. During repetition of such steps, the test results of the outer loop were never fed back to the classifier's optimization process in the inner loops, and hence the tests in the outer loop did not include any overestimation, and the estimated accuracy involved the smallest bias as possible.

The posterior value for a single sample was calculated based on the distribution of the weighted vote (decision by majority by the genes that join the vote) *f* within the LTO analysis. We regard a real-valued weighted vote as carrying two kinds of information: its sign predicts the label (favorable or unfavorable) of the corresponding sample, and its absolute value shows the prediction strength. The posterior probability p for this sample being favorable (alive at 5 years) was evaluated as the logit transformation $p = \exp(\beta_0 + \beta_1 f)/[1 + \exp(\beta_0 + \beta_1 f)]$, where parameters β_0 and β_1 were estimated by the maximum likelihood method, in each step in the outer loop of LTO using the remaining 95 samples and the corresponding labels (5 year prognosis). Then, the posterior probability of the sample left out in the outer loop was predicted by the weighted vote *f* by the classifier constructed in the inner LOO loops and the parameters β_0 and β_1 obtained above. There is therefore no information leakage in this calculation process of the posterior of the sample left out.

Independent test

Using the 50 independent samples, we performed two kinds of tests. The first one is an independent test to validate the classifier obtained by our method and the applicability of our classifier to the mini-chip system, which has been developed as a clinical tool at the bedside (Figure S2B). According to the LTO analysis, the supervised classifier was finally constructed by using all of the 96 training samples measured by the 5340 genes system. This classifier was evaluated by being directly applied to the 50 samples measured by the mini-chip system without any information from measurements by the mini-chip system and the 50 test samples. In this test, tumor RNA preparation, probe labeling, and hybridization were conducted in a completely different laboratory from that for the 5340 genes system. The second one is to validate the LTO analysis to construct a supervised classifier by applying the procedure to the data taken by the mini-chip system.

Survival analysis

The Kaplan-Meier survival analysis was also programmed and used to compare patient survival. To assess the association of selected gene expression with patient clinical outcome, the statistical p and q values were calculated based on the log rank test.

Immunohistochemistry

Immunostaining with the antibody against peripherin protein (Santa Cruz Biotechnology; 1:400) was performed on six human neuroblastoma tumors selected from the surgical pathology file at the Department of Pathology, Aichi Medical University. They were all neuroblastoma (Schwannian stroma–poor) and included three favorable histology tumors (poorly differentiated subtype without *MYCN* amplification [one case]; differentiated subtype without *MYCN* amplification [two cases]) and three unfavorable histology tumors (undifferentiated subtype without *MYCN* amplification [one case]; poorly differentiated subtype with *MYCN* amplification [one case]; poorly differentiated subtype without *MYCN* amplification). All tumor tissues were obtained prior to chemotherapy and irradiation therapy. Four micron thick sections from the formalin-fixed, paraffin-embedded samples of these tumors were treated according to the protocol described previously (Kato et al., 2004). As for the negative controls, normal goat immunoglobulins (1:500 dilution; Vector Laboratories) were applied as the primary antibody.

Supplemental data

The Supplemental Data include Supplemental Experimental Procedures and ten supplemental figures and can be found with this article online at http://www.cancercell.org/cgi/content/full/7/4/337/DC1/.

Acknowledgments

We are grateful to the hospitals and institutions that provided us with surgical specimens (see the Supplemental Data). We also thank Shigeru Sakiyama and John K. Cowell for reading the manuscript; Naohiko Seki, Tsutomu Yoshikawa, and Masaki Kato for their valuable suggestions; and Natsue Kitabayashi, Tomonori Saito, Naoko Sugimitsu, Yuki Nakamura, Naoko Shibano, Emiko Kojima, Hisae Murakami, and Kazumi Yagyu for their technical support. This work was supported in part by a fund from Hisamitsu Pharmaceutical Co., Inc.; by Grants-in-Aid for Scientific Research on Priority Areas (C) "Medical Genome Science" and "Genome Information Science" and for Scientific Research (B) from the Ministry of Education, Culture, Sports, Science and Technology of Japan; and by Grant-in Aid for Cancer Research from the Ministry of Health, Labor and Welfare of Japan.

Received: November 17, 2003
Revised: January 8, 2005
Accepted: March 11, 2005
Published: April 18, 2005

References

Aletta, J.M., Shelanski, M.L., and Greene, L.A. (1989). Phosphorylation of the peripherin 58-kDa neuronal intermediate filament protein. J. Biochem. (Tokyo) *264*, 4619–4627.

Ambros, I.M., and Ambros, P.F. (1995). Schwann cells in neuroblastoma. Eur. J. Cancer *4*, 429–434.

Ambros, I.M., and Ambros, P.F. (2000). The role of Schwann cells in neuroblastoma. In Neuroblastoma, G.M. Brodeur, T. Sawada, Y. Tsuchida, and P.A. Voute, eds. (Amsterdam: Elsevier), pp. 229–243.

Beer, D.G., Kardia, S.L., Huang, C.C., Giordano, T.J., Levin, A.M., Misek, D.E., Lin, L., Chen, G., Gharib, T.G., Thomas, D.G., et al. (2002). Gene-expression profiles predict survival of patients with lung adenocarcinoma. Nat. Med. *8*, 816–824.

Berwanger, B., Hartmann, O., Bergmann, E., Bernard, S., Nielsen, D., Krause, M., Kartal, A., Flynn, D., Wiedemeyer, R., Schwab, M., et al. (2002). Loss of a FYN-regulated differentiation and growth arrest pathway in advanced stage neuroblastoma. Cancer Cell *2*, 377–386.

Bo, T., and Jonassen, I. (2002). New feature subset selection procedures for classification of expression profiles. Genome Biol. *3*, RESEARCH0017.

Bolande, R.P. (1974). The neurocristopathies: a unifying concept of disease arising in neural crest maldevelopment. Hum. Pathol. *5*, 409–429.

Brodeur, G.M., and Nakagawara, A. (1992). Molecular basis for clinical heterogeneity in neuroblastoma. Am. J. Pediatr. Hematol. Oncol. *14*, 111–116.

Brodeur, G.M., Seeger, R.C., Schwab, M., Varmus, H.E., and Bishop, J.M.

(1984). Amplification of N-myc in untreated human neuroblastomas correlates with advanced disease stage. Science *224*, 1121–1124.

Brodeur, G.M., Fong, C.T., Morita, M., Griffith, R., Hayes, F.A., and Seeger, R.C. (1988). Molecular analysis and clinical significance of N-myc amplification and chromosome 1p monosomy in human neuroblastomas. Prog. Clin. Biol. Res. *271*, 3–15.

Brodeur, G.M., Pritchard, J., Berthold, F., Carlsen, N.L., Castel, V., Castelberry, R.P., De Bernardi, B., Evans, A.E., Favrot, M., Hedborg, F., et al. (1993). Revisions of the international criteria for neuroblastoma diagnosis, staging, and response to treatment. J. Clin. Oncol. *11*, 1466–1477.

Ceci, M., Gaviraghi, C., Gorrini, C., Sala, L.A., Offenhauser, N., Marchisio, P.C., and Biffo, S. (2003). Release of eIF6 (p27BBP) from the 60S subunit allows 80S ribosome assembly. Nature *426*, 579–584.

Chomczynski, P., and Sacchi, N. (1987). Single-step method of RNA isolation by acid guanidinium thiocyanate-phenol-chloroform extraction. Anal. Biochem. *162*, 156–159.

Cleveland, W.S. (1979). Robust locally weighted regression and smoothing scatterplots. J. Am. Stat. Assoc. *74*, 829–836.

Evans, A.E., D'Angio, G.J., and Randolph, J. (1971). A proposed staging for children with neuroblastoma. Children's cancer study group A. Cancer *27*, 374–378.

Favrot, M.C., Combaret, V., and Lasset, C. (1993). CD44—a new prognostic marker for neuroblastoma. N. Engl. J. Med. *329*, 1965.

Godbout, R., and Squire, J. (1993). Amplification of a DEAD box protein gene in retinoblastoma cell lines. Proc. Natl. Acad. Sci. USA *90*, 7578–7582.

Golub, T.R., Slonim, D.K., Tamayo, P., Huard, C., Gaasenbeek, M., Mesirov, J.P., Coller, H., Loh, M.L., Downing, J.R., Caligiuri, M.A., et al. (1999). Molecular classification of cancer: class discovery and class prediction by gene expression monitoring. Science *286*, 531–537.

Hall, J.L., and Cowan, N.J. (1985). Structural features and restricted expression of a human α-tubulin gene. Nucleic Acids Res. *13*, 207–223.

Hishiki, T., Nimura, Y., Isogai, E., Kondo, K., Ichimiya, S., Nakamura, Y., Ozaki, T., Sakiyama, S., Hirose, M., Seki, N., et al. (1998). Glial cell line-derived neurotrophic factor/neurturin-induced differentiation and its enhancement by retinoic acid in primary human neuroblastomas expressing c-Ret, GFR α-1, and GFR α-2. Cancer Res. *58*, 2158–2165.

Hiyama, E., Hiyama, K., Yokoyama, T., Matsuura, Y., Piatyszek, M.A., and Shay, J.W. (1995). Correlating telomerase activity levels with human neuroblastoma outcomes. Nat. Med. *1*, 249–255.

Iizuka, N., Oka, M., Yamada-Okabe, H., Nishida, M., Maeda, Y., Mori, N., Takao, T., Tamesa, T., Tangoku, A., Tabuchi, H., et al. (2003). Oligonucleotide microarray for prediction of early intrahepatic recurrence of hepatocellular carcinoma after curative resection. Lancet *361*, 923–929.

Kaneko, M., Nishihira, H., Mugishima, H., Ohnuma, N., Nakada, K., Kawa, K., Fukuzawa, M., Suita, S., Sera, Y., and Tsuchida, Y. (1998). Stratification of treatment of stage 4 neuroblastoma patients based on N-myc amplification status. Study Group of Japan for Treatment of Advanced Neuroblastoma, Tokyo, Japan. Med. Pediatr. Oncol. *31*, 1–7.

Kato, C., Miyazaki, K., Nakagawa, A., Ohira, M., Nakamura, Y., Ozaki, T., Imai, T., and Nakagawara, A. (2004). High expression of human tubulin tyrosine ligase and enhanced tubulin tyrosination/detyrosination cycle are associated with neuronal differentiation in neuroblastomas with favorable prognosis. Int. J. Cancer *112*, 365–375.

Knoops, B., and Octave, J.N. (1997). α1-tubulin mRNA level is increased during neurite outgrowth of NG 108-15 cells but not during neurite outgrowth inhibition by CNS myelin. Neuroreport *8*, 795–798.

Look, A.T., Hayes, F.A., Nitschke, R., McWilliams, N.B., and Green, A.A. (1984). Cellular DNA content as a predictor of response to chemotherapy in infants with unresectable neuroblastoma. N. Engl. J. Med. *311*, 231–235.

Look, A.T., Hayes, F.A., Shuster, J.J., Douglass, E.C., Castleberry, R.P., Bowman, L.C., Smith, E.I., and Brodeur, G.M. (1991). Clinical relevance of tumor cell ploidy and N-myc gene amplification in childhood neuroblastoma: a Pediatric Oncology Group study. J. Clin. Oncol. *9*, 581–591.

Nagata, T., Takahashi, Y., Asai, S., Ishii, Y., Mugishima, H., Suzuki, T., Chin, M., Harada, K., Koshinaga, S., and Ishikawa, K. (2000). The high level of hCDC10 gene expression in neuroblastoma may be associated with favorable characteristics of the tumor. J. Surg. Res. *92*, 267–275.

Nakagawara, A., Arima, M., Azar, C.G., Scavarda, N.J., and Brodeur, G.M. (1992). Inverse relationship between trk expression and N-myc amplification in human neuroblastomas. Cancer Res. *52*, 1364–1368.

Nakagawara, A., Arima-Nakagawara, M., Scavarda, N.J., Azar, C.G., Cantor, A.B., and Brodeur, G.M. (1993). Association between high levels of expression of the TRK gene and favorable outcome in human neuroblastoma. N. Engl. J. Med. *328*, 847–854.

Nakagawara, A., Milbrandt, J., Muramatsu, T., Deuel, T.F., Zhao, H., Cnaan, A., and Brodeur, G.M. (1995). Differential expression of pleiotrophin and midkine in advanced neuroblastomas. Cancer Res. *55*, 1792–1797.

Noguchi, T., Akiyama, K., Yokoyama, M., Kanda, N., Matsunaga, T., and Nishi, Y. (1996). Amplification of a DEAD box gene (DDX1) with the MYCN gene in neuroblastomas as a result of cosegregation of sequences flanking the MYCN locus. Genes Chromosomes Cancer *15*, 129–133.

Ntzani, E.E., and Ioannidis, J.P. (2003). Predictive ability of DNA microarrays for cancer outcomes and correlates: an empirical assessment. Lancet *362*, 1439–1444.

Oba, S., Takemasa, N., Monden, M., Matsubara, K., and Ishii, S. (2003). A Bayesian missing value estimation method. Bioinformatics *19*, 2088–2096.

Ohira, M., Morohashi, A., Inuzuka, H., Shishikura, T., Kawamoto, T., Kageyama, H., Nakamura, Y., Isogai, E., Takayasu, H., Sakiyama, S., et al. (2003a). Expression profiling and characterization of 4200 genes cloned from primary neuroblastomas: identification of 305 genes differentially expressed between favorable and unfavorable subsets. Oncogene *22*, 5525–5536.

Ohira, M., Morohashi, A., Nakamura, Y., Isogai, E., Furuya, K., Hamano, S., Machida, T., Aoyama, M., Fukumura, M., Miyazaki, K., et al. (2003b). Neuroblastoma oligo-capping cDNA project: toward the understanding of the genesis and biology of neuroblastoma. Cancer Lett. *197*, 63–68.

Sawada, T., Hirayama, M., Nakata, T., Takeda, T., Takasugi, N., Mori, T., Maeda, K., Koide, R., Hanawa, Y., Tsunoda, A., et al. (1984). Mass screening for neuroblastoma in infants in Japan. Interim report of a mass screening study group. Lancet *2*, 271–273.

Schwab, M., Alitalo, K., Klempnauer, K.H., Varmus, H.E., Bishop, J.M., Gilbert, F., Brodeur, G., Goldstein, M., and Trent, J. (1983). Amplified DNA with limited homology to myc cellular oncogene is shared by human neuroblastoma cell lines and a neuroblastoma tumour. Nature *305*, 245–248.

Shimada, H., Chatten, J., Newton, W.A., Sachs, N., Hamoudi, A.B., Chiba, T., Marsden, H.B., and Misugi, K. (1984). Histopathologic prognostic factors in neuroblastic tumors; definition of subtypes of ganglioneuroblastoma and an age-linked classification of neuroblastomas. J. Natl. Cancer Inst. *73*, 405–416.

Shimono, R., Matsubara, S., Takamatsu, H., Fukushige, T., and Ozawa, M. (2000). The expression of cadherins in human neuroblastoma cell lines and clinical tumors. Anticancer Res. *20*, 917–923.

Slavc, I., Ellenbogen, R., Jung, W.H., Vawter, G.F., Kretschmar, C., Grier, H., and Korf, B.R. (1990). myc gene amplification and expression in primary human neuroblastoma. Cancer Res. *50*, 1459–1463.

Storey, J.D., and Tibshirani, R. (2003). Statistical significance for genome-wide studies. Proc. Natl. Acad. Sci. USA *100*, 9440–9445.

Takahashi, M., Seki, N., Ozaki, T., Kato, M., Kuno, T., Nakagawa, T., Watanabe, K., Miyazaki, K., Ohira, M., Hayashi, S., et al. (2002). Identification of the p33(ING1)-regulated genes that include cyclin B1 and proto-oncogene DEK by using cDNA microarray in a mouse mammary epithelial cell line NMuMG. Cancer Res. *62*, 2203–2209.

Ueda, K. (2001). Detection of the retinoic acid-regulated genes in a RTBM1 neuroblastoma cell line using cDNA microarray. Kurume Med. J. *48*, 159–164.

van 't Veer, L.J., Dai, H., van de Vijver, M.J., He, Y.D., Hart, A.A., Mao, M., Peterse, H.L., van der Kooy, K., Marton, M.J., Witteveen, A.T., et al. (2002). Gene expression profiling predicts clinical outcome of breast cancer. Nature *415*, 530–536.

Yamanaka, Y., Hamazaki, Y., Sato, Y., Ito, K., Watanabe, K., Heike, T., Nakahata, T., and Nakamura, Y. (2002). Maturational sequence of neuroblastoma revealed by molecular analysis on cDNA microarrays. Int. J. Oncol. *21*, 803–807.

Yoshikawa, T., Nagasugi, Y., Azuma, T., Kato, M., Sugano, S., Hashimoto, K., Masuho, Y., Muramatsu, M., and Seki, N. (2000). Isolation of novel mouse genes differentially expressed in brain using cDNA microarray. Biochem. Biophys. Res. Commun. *275*, 532–537.

Accession numbers

Microarray data are available at NCBI Gene Expression Omnibus (accession number GSE2283).

American Journal of Pathology, Vol. 167, No. 1, July 2005
Copyright © American Society for Investigative Pathology

Tumorigenesis and Neoplastic Progression

Biological Role of Anaplastic Lymphoma Kinase in Neuroblastoma

Yuko Osajima-Hakomori,*¶‖ Izumi Miyake,*† Miki Ohira,‡ Akira Nakagawara,‡ Atsuko Nakagawa,§ and Ryuichi Sakai*

From the Growth Factor Division, National Cancer Center Research Institute, Chuo-ku, Tokyo; St. Marianna University School of Medicine,¶ Kawasaki-shi, Kanagawa; Tokyo Metropolitan Geriatric Hospital,‖ Itabashi-ku, Tokyo; the Department of Pediatrics,† Kitasato University School of Medicine, Sagamihara-shi, Kanagawa; the Division of Biochemistry,‡ Chiba Cancer Center Research Institute, Cyuo-ku, Chiba; and the Department of Pathology,§ Aichi Medical University, Aichi-gun, Aichi, Japan*

Anaplastic lymphoma kinase (ALK) is a tyrosine kinase receptor originally identified as part of the chimeric nucleophosmin-ALK protein in the t(2;5) chromosomal rearrangement associated with anaplastic large cell lymphoma. We recently demonstrated that the ALK kinase is constitutively activated by gene amplification at the ALK locus in several neuroblastoma cell lines. Forming a stable complex with hyperphosphorylated ShcC, activated ALK modifies the responsiveness of the mitogen-activated protein kinase pathway to growth factors. In the present study, the biological role of activated ALK was examined by suppressing the expression of ALK kinase in neuroblastoma cell lines using an RNA interference technique. The suppression of activated ALK in neuroblastoma cells by RNA interference significantly reduced the phosphorylation of ShcC, mitogen-activated protein kinases, and Akt, inducing rapid apoptosis in the cells. By immunohistochemical analysis, the cytoplasmic expression of ALK was detected in most of the samples of neuroblastoma tissues regardless of the stage of the tumor, whereas significant amplification of ALK was observed in only 1 of 85 cases of human neuroblastoma samples. These data demonstrate the limited frequency of ALK activation in the real progression of neuroblastoma. *(Am J Pathol 2005, 167:213–222)*

Receptor tyrosine kinases (RTKs) play an important role in regulating diverse cellular processes, such as proliferation, differentiation, survival, motility, and malignant transformation. The activation of RTKs typically requires ligand-induced receptor oligomerization, which results in tyrosine autophosphorylation of the receptors at tyrosine residues.[1–3] By recruiting specific sets of signal transducer molecules in a phosphorylation-dependent manner, each RTK is capable of inducing individual, specific cellular responses.[4] On the other hand, activation of RTKs by either mutations or overexpression is frequently found in various human malignancies.[3,5]

Anaplastic lymphoma kinase (ALK) is a 200-kd tyrosine kinase encoded by the *ALK* gene on chromosome 2p23. ALK was first identified as part of an oncogenic fusion tyrosine kinase, nucleophosmin-ALK, which is associated with anaplastic large cell lymphoma.[6,7] It was also found as a form of fusion protein with a clathrin heavy chain (CTCL) in myofibroblastic tumors.[8] Full-length ALK has the typical structure of an RTK, with a large extracellular domain, a lipophilic transmembrane segment, and a cytoplasmic tyrosine kinase domain.[9,10] ALK is highly homologous to leukocyte tyrosine kinase (LTK) and is further classified into the insulin receptor superfamily. The *LTK* gene is mainly expressed in pre-B lymphocytes and neuronal tissues,[11–13] whereas expression of the normal *ALK* gene in hematopoietic tissues has not been detected. Instead, it is dominantly expressed in the neural system.[14,15] In the developing brains of mice, specific expression of *ALK* was seen in the thalamus, mid-brain, olfactory bulb, and selected cranial regions, as well as the dorsal root, the ganglia of mice,[9,10,16] suggesting a specific role in the development of the embryonic nervous system. Currently, however, the function of ALK in adult normal tissue or carcinogenesis remains an open question. Several studies have recently indicated pleiotrophin or midkine as possible ligands for ALK.[17,18] Although they appeared to induce the functional activa-

Supported by the Program for the Promotion of Fundamental Studies in Health Science of the Organization for Pharmaceutical Safety and Research of Japan. Y.O-H. is the recipient of a Research Resident Fellowship from the Foundation for Promotion of Cancer Research, Japan.

Accepted for publication March 23, 2005.

Address reprint requests to Ryuichi Sakai, M.D., Growth Factor Division, National Cancer Center Research Institute, 5-1-1 Tsukiji, Chuo-ku, Tokyo 104-0045, Japan. E-mail: rsakai@gan2.res.ncc.go.jp.

tion of ALK, it is still unclear whether these molecules are the physiological ligands of ALK.

Neuroblastoma is one of the most common pediatric tumors derived from the sympathoadrenal linage of the neural crest. Tumors found in patients under the age of 1 year are usually favorable and often show spontaneous differentiation and regression.[19] Amplification of the N-*myc* gene occurs in approximately 25% of neuroblastomas and correlates with the aggressiveness of the disease. In addition to N-*myc* gene amplification, the expression of various genes has significant correlation with the stage of and prognosis for neuroblastoma. A high level of TrkA expression is predictive of a favorable outcome,[20] whereas TrkB is highly expressed in immature neuroblastomas with N-*myc* amplification.[21] High expression of caspase-1, -3, and -8 is correlated with favorable neuroblastomas.[22,23] On the other hand, survivin, which suppresses caspase and promotes the cell survival signal, is significantly expressed,[24] and telomerase is activated[25] in unfavorable tumors. There may be a critical difference in the expression of other molecules, including RTKs, in neuroblastoma. A recent paper showed that full-length ALK is detected in almost one-half of the cell lines derived from neuroblastomas and neuroectodermal tumors.[26] We have recently shown using mass-spectrometry analysis that ALK is a major phosphoprotein associated with hyperphosphorylated ShcC in several neuroblastoma cell lines.[27] In these cells, ALK was markedly activated, and it induced the constitutive phosphorylation of ShcC and mitogen-activated protein kinase (MAPK), regardless of stimulation by epidermal growth factor (EGF) or nerve growth factor.[27] These findings strongly suggest that constitutively activated ALK kinase plays a physiological role in the development of neuroblastoma.

In this study, we investigated the biological function of the constitutively activated ALK kinase in neuroblastoma. The RNA interference (RNAi) technique using specific sets of small interfering RNA (siRNA) was induced to inhibit the *ALK* gene expression in human neuroblastoma cells with or without gene amplification of *ALK*. The effects of disrupted ALK expression on cell survival or downstream signaling, such as MAPKs or Akt pathways, are examined to understand the biological meaning of ALK amplification in neuroblastoma cells. We also performed Southern blot analysis of primary neuroblastoma tumors from 85 patients to check whether the *ALK* gene amplification was actually present in neuroblastoma tissues. Furthermore, we sought the *ALK* gene expression in human neuroblastoma tissues using immunohistochemical analysis.

Materials and Methods

Cell Culture

Cell lines of human neuroblastoma were maintained in RPMI 1640 supplemented with 10% fetal calf serum (Sigma, St. Louis, MO), penicillin, and streptomycin at 37°C in a humidified 5% CO_2 incubator.

Reverse Transcription-Polymerase Chain Reaction (RT-PCR) Analysis

Total RNA was extracted with ISOGEN (Nippongene Japan, Toyama, Japan) from NB-39-nu and SK-N-MC cells. The PCR primer pair 5′-AGGTTCTGGCTGCAGATGGT-3′ and 5′-ACATTGTTCTCTCGAGTGCAGAC-3′ corresponding to the cytoplasmic portion of human ALK was prepared. As much as 0.25 μg of total RNA was reverse transcribed and amplified with the SuperScript One-step RT-PCR with the Platinum *Taq* kit (Invitrogen Life Technologies, Carlsbad, CA) in a total volume of 50l including 2× reaction mix, 0.2 μmol/L of each primer, and 1 μl of RT/Platinum *Taq* Mix. Amplification conditions consisted of cDNA synthesis and predenaturation at 50°C for 30 minutes and 94°C for 2 minutes followed by 25 cycles at 94°C for 15 seconds, 58°C for 30 seconds, and 72°C for 45 seconds. A final amplification for 7 minutes at 72°C finished the PCR. The product was separated with 1.2% agarose gel electrophoresis and analyzed using the Quality One System (Bio-Rad, Hercules, CA).

Immunochemical Analysis of Proteins

Immunoprecipitation and immunoblotting were performed as described previously.[27] The polyclonal antibodies against the CH1 domains of ShcC (amino acids 306–371) and the anti-ALK antibody (αALK) that was against the cytoplasmic portion (amino acid 1379–1524) of human ALK were prepared as described previously.[27,28] An anti-phosphotyrosine antibody (4G10) was obtained from UBI. Anti-p44/42 MAPKs, anti-phospho-p44/42 MAPKs, anti-Akt, and anti-phospho-Akt antibodies were purchased from Cell Signaling (Beverly, MA). Anti-EGF receptor (EGFR), anti-Ret, and anti-TrkA antibodies were purchased from Santa Cruz Biotechnology (Santa Cruz, CA). *In vitro* kinase assay for ALK was performed as previously described.[27] Anti-ALK immunoprecipitates were incubated with or without Poly-Glu/Tyr as an exogenous substrate.

Immunocytostaining

For ALK/TOTO-3, immunostaining using anti-ALK antibody was performed at first, and then nuclei were stained using TOTO-3. The cells seeded on the 24-well plates were washed with phosphate-buffered saline (PBS) three times and fixed with 4% paraformaldehyde (methanol free) for 5 minutes at room temperature. The cells were rinsed with PBS twice and then permeabilized with 0.2% Triton X-100 solution in PBS for 10 minutes at room temperature. The cells were blocked with 5% goat serum and 3% bovine serum albumin–Tris-buffered saline for 30 minutes at room temperature. The blocking solution was drained off, and the cells were incubated with a 1:1000 dilution of αALK for 1 hour at room temperature. The cells were rinsed with PBS three times and incubated with a 1:2000 dilution of Alexa fluor (Molecular Probes, Eugene, OR) and 1: 100 dilution of TOTO-3 (Molecular Probes) for

Table 1. Patient Characteristics of Neuroblastoma Tissues with *ALK* Gene Gain or Amplification

Case	Age*	Primary tumor		Copy nos. of *ALK*‡	Amplification of N-*myc* (*n*)
		Location	Clinical stage†		
1	3y5m	Adrenal gland	IV	2.0 ± 0.2	+ (35)
2	5y0m	Peritoneum	IV	1.8 ± 0.1	+ (>150)
3	2y7m	Abdomen	IV	2.1 ± 0.8	+ (150)
4	8m	Adrenal gland	I	3.0 ± 1.0	−
5	4y9m	Abdomen	IV	2.0 ± 0.2	−
6	3y9m	Adrenal gland	III	2.7 ± 0.2	+ (>150)
7	1y4m	Adrenal gland	IV	2.8 ± 1.0	+ (150)
8	1y7m	Adrenal gland	IV	9.5 ± 2.2	+ (>100)

*Age of onset: year (y), month (m).
†The staging criterion was based on the International Neuroblastoma Staging System.
‡The averages of the calculated copy numbers from three independent blottings are shown.

30 minutes at room temperature. The cells were washed three times with PBS and mounted in glycerol-based 2.5% 1,4-diazabicyclo[2,2,2] octan. Confocal laser scanning analysis was carried out. For ALK/TUNEL, we first carried out TUNEL and then proceeded to standard immunocytochemistry using anti-ALK antibody. TUNEL was performed using the DeadEnd Fluorometric TUNEL System (Promega, Madison, WI) with the following modifications. The NB-39-nu cells seeded on the 24-well plates that were treated with siRNAs were washed with PBS twice and fixed with 4% paraformaldehyde (methanol free) for 25 minutes at 4°C. The cells were rinsed with PBS twice and then permeabilized with 0.2% Triton X-100 solution in PBS for 5 minutes at room temperature. The cells were washed with PBS twice and covered with an equilibration buffer (from the kit) for 10 minutes at room temperature. The equilibration buffer was drained off, and a reaction buffer containing the equilibration buffer, nucleotide mix, and terminal deoxynucleotidyl transferase enzyme was added to the cells and incubated at 37°C for 1 hour, avoiding exposure to light. The cells were incubated for 15 minutes at room temperature with 2× standard saline citrate to stop the reaction. The cells were washed with PBS three times and then stained for ALK using immunofluorescence as follows. The cells were blocked with 2% bovine serum albumin (Boehringer Mannheim, Germany) for 30 minutes at room temperature. The blocking solution was drained off, and the cells were incubated with a 1:1000 dilution of αALK for 1 hour at room temperature. The cells were rinsed with PBS three times and incubated with a 1:40 dilution of rhodamine-conjugated goat anti-rabbit secondary antibody (Santa Cruz Biotechnology) for 30 minutes at room temperature. The cells were washed three times with PBS and then mounted and observed in the same manner as that for ALK/TOTO-3.

DNA Extraction and Southern Blotting

Genomic DNAs derived from neuroblastoma cell lines were obtained from cultured cells as described using the procedure of Perucho et al.[29] Samples of 85 neuroblastoma tissues were collected at the Chiba Cancer Center and stored as forms of genomic DNA. The characteristics of some of these patients are shown in Table 1. The stage criterion was based on the International Neuroblastoma Staging System.[30] Samples of 5 μg of DNA digested by *Eco*RI were electrophoresed in 0.8% agarose gel and blotted onto nitrocellulose filters (Hybond-N+; Amersham, Piscataway, NJ). The probes for detecting the *ALK* gene, N-*myc* gene, and *ShcC* gene were used in our previous study.[27] The intensities of these signals were measured using a Molecular Imager FxPro (Bio-Rad). This study was approved by the ethical judging committee of the National Cancer Center and the Chiba Cancer Center of Japan.

RNA Interference Technique

Twenty-one-nucleotide double-stranded RNAs were synthesized and purified using Dharmacon Research (Lafayette, CO). To suppress the expression of ALK protein, two different pairs of ALK siRNAs, ALK-siRNA1 and ALK-siRNA2, were obtained. The sequences were 5′-GAGUCUGGCAGUUGACUUCdTdT-3′ for ALK-siRNA1 and 5′-GCUCCGGCGUGCCAAGCAGdTdT-3′ for ALK-siRNA2, corresponding to coding region 153 to 171 and 399 to 417 relative to the first nucleotide of the start codon, respectively. Entire sequences were derived from the sequence of human *ALK* mRNA (accession no. HSU62540). An siRNA, targeting a sequence in the firefly (*Photinus pyralis*) luciferase mRNA, was used as a negative control (Dharmacon) (luc-siRNA). We also used a scramble siRNA, Scramble Duplex II (Dharmacon) (s-siRNA) as a mismatch siRNA control in addition to luc-siRNA.

NB-39-nu cells were trypsinized, diluted with growth medium containing 10% fetal calf serum, and transferred to 12-well plates at 6×10^4 cells per well for 24 hours before transfection. The transfection of siRNA was carried out using jetSI (Poly plus transfection). A total of 100 μl of serum-free growth medium and 4 μl of jetSI per well were preincubated for 5 to 10 minutes at room temperature. While the incubation was being performed, 100 μl of serum-free growth medium was mixed with 5 μl of 20 μmol/L siRNA duplex (100 pmol). Total siRNA amounts of 50, 100, and 200 pmol were checked in preliminary experiments to find out 100 pmol is the minimal and optimal amount in this scale of RNAi. The 100 μl of jetSI serum-free medium solution was added to the 100 μl of siRNA

duplex solution, gently mixed, and incubated for 30 minutes at room temperature. The growth medium on the cells was removed, and 800 μl of serum-free medium was added to each well. A total of 200 μl of the entire mixture was overlaid onto the cells, and cells were incubated for 4 hours at 37°C in a 5% CO_2 incubator. After incubation, 1 ml of medium containing 4% fetal calf serum was added without removing the transfection mixture (final concentration 2%). The cells were assayed 84 hours after transfection. SK-N-MC cells were seeded in 12-well plates at a concentration of 1.3×10^5 cells per well. These were treated with siRNAs in the same way as NB-39-nu and assayed 48 hours after transfection. In the 24-well plate, the cells were seeded at the same concentration as the 12-well plate, and siRNAs and all other reagents were used at half volume. After transfection, the cells were examined under a light microscope every day.

Double Staining for ALK and TUNEL

For double staining, we first carried out TUNEL and then proceeded to standard immunocytochemistry using anti-ALK antibody. TUNEL was performed using the DeadEnd Fluorometric TUNEL System (Promega) with the following modifications. The NB-39-nu cells seeded on the 24-well plates that were treated with siRNAs were washed with PBS twice and fixed with 4% paraformaldehyde (methanol free) for 25 minutes at 4°C. The cells were rinsed with PBS twice and then permeabilized with 0.2% Triton X-100 solution in PBS for 5 minutes at room temperature. The cells were washed with PBS twice and covered with an equilibration buffer (from the kit) for 10 minutes at room temperature. The equilibration buffer was drained off, and a reaction buffer containing the equilibration buffer, nucleotide mix, and terminal deoxynucleotidyl transferase enzyme was added to the cells and incubated at 37°C for 1 hour, avoiding exposure to light. The cells were incubated for 15 minutes at room temperature with 2× standard saline citrate to stop the reaction. The cells were washed with PBS three times and then stained for ALK using immunofluorescence as follows. The cells were blocked with 2% bovine serum albumin (Boehringer Mannheim) for 30 minutes at room temperature. The blocking solution was drained off, and the cells were incubated with a 1:1000 dilution of αALK for 1 hour at room temperature. The cells were rinsed with PBS three times and incubated with a 1:40 dilution of rhodamine-conjugated goat anti-rabbit secondary antibody (Santa Cruz Biotechnology) for 30 minutes at room temperature. The cells were washed three times with PBS and mounted in glycerol-based 2.5% 1,4-diazabicyclo[2,2,2] octan. Confocal laser scanning analysis was carried out.

DNA Fragmentation Assay

To detect apoptotic DNA cleavage, DNA fragmentation assay was performed using an Apoptotic DNA Ladder kit (Chemicon International, Inc., Temecula, CA). The cells seeded on the 12-well plates that were treated with siRNAs as previously mentioned were collected in 1.5-ml microcentrifuge tubes. The cells were washed with PBS, centrifuged, and lysed with 20 μl of TE lysis buffer. The lysates were incubated with 5 μl of enzyme A (RNase A) at 37°C for 10 minutes and then at 55°C for 30 minutes after the addition of 5 μl of Enzyme B (Proteinase K). Afterward, 5 μl of ammonium acetate solution and 100 μl of absolute ethanol were added, and the samples were kept at −20°C for 10 minutes. The samples were centrifuged, and the pellets were washed with 70% ethanol. Then the DNA pellets were dissolved in 30 μl of DNA suspension buffer. DNA fragmentations were visualized by electrophoresis on 2% agarose gel containing ethidium bromide.

Immunohistochemistry

As for positive control, tumor xenograft was made by injection of NB-39-nu cells subcutaneously in 5-week-old SCID mice. Immunohistochemical staining with ALK antibody (αALK) (1:1000), was performed on 16 human neuroblastoma tumors selected from the surgical pathology file at the Department of Pathology, Aichi Medical University based on the results of histopathology evaluation[31] and N-*myc* status. All of those tumor samples were obtained before chemotherapy and irradiation therapy and included nine favorable histology cases with nonamplified N-*myc* (FH&NA), two unfavorable histology cases with amplified N-*myc* (UH&A), and five unfavorable histology cases with nonamplified N-*myc* (UH&NA).

Four-micrometer-thick sections from the formalin-fixed and paraffin-embedded tissue samples were deparaffinized and microwaved for three times for 5 minutes in Na-citrate buffer (pH 6.0) for antigen retrieval. The slides were first immersed in 0.3% hydrogen peroxide in methanol for 20 minutes and then in 10% normal goat serum for 30 minutes. The primary antibody (αALK) was then applied at 4°C overnight, followed by a standard staining procedure using the Vectastain ABC kit (Vector Laboratories, Burlingame, CA). Sections were counterstained with hematoxylin for light microscopic review and evaluation. ALK was always positively detected in the cytoplasm of NB-39-nu tumor xenograft and in the cytoplasm and neuritic processes of normal ganglion cells in the separate positive control sections as well as in the test sections as built-in control, whenever available. As for the negative controls, normal rabbit immunoglobulins (1:500 dilution; Vector Laboratories) or preimmune serum for α ALK (1:1000 dilution) was applied as the primary antibody.

Results

Significant Amplification of the ALK Gene and Constitutive Activation of ALK Kinase in Three Neuroblastoma Cell Lines

As shown in Figure 1A, NB-39-nu, Nagai, and NB-1 cells have significant levels of amplification of the *ALK* gene (30–40 copies per cell) among 25 neuroblastoma and neuroepithelioma cell lines examined. Other cell lines such as SK-N-MC have only one copy of the *ALK* gene just like the

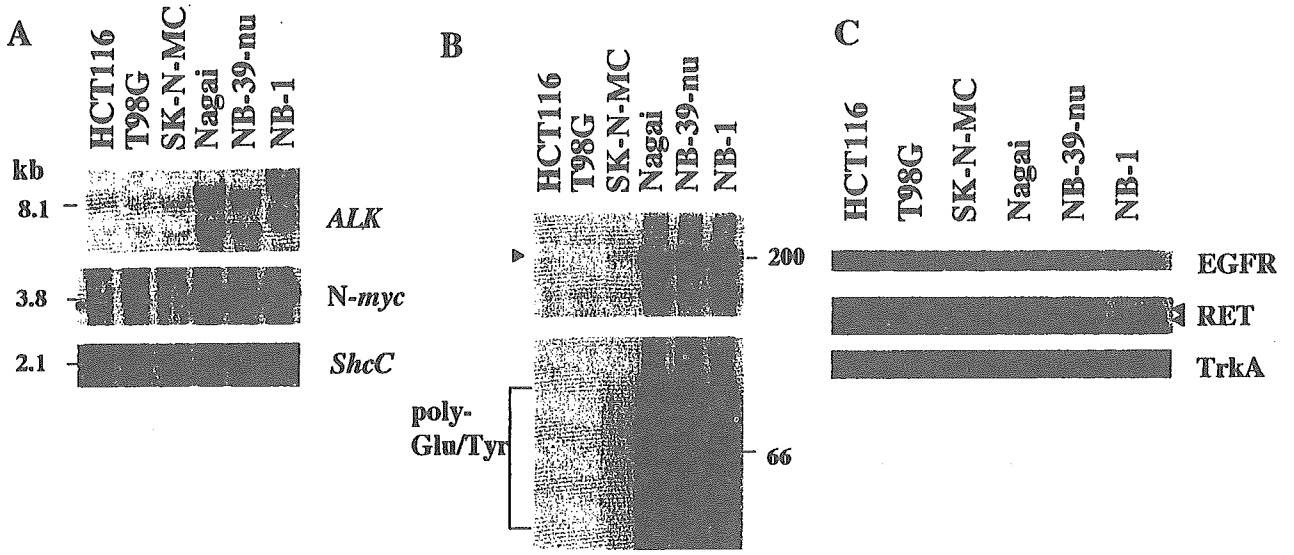

Figure 1. Marked gene amplification of the *ALK* locus and significant elevation of kinase activity of ALK in NB-39-nu, Nagai, and NB-1 cells. **A:** To detect ALK gene amplification, samples of 10 μg of DNA were digested with *Eco*RI. Fragments of about 2.5, 3.1, 6.1, and 8.1 kb were detected using the ^{32}P-labeled probe prepared as previously described.[27] Amplification of the N-*myc* gene was detected using the same filter re-hybridized with the probe for N-*myc*. As a control for the amounts of DNA, the same filter was re-hybridized with the probe for *ShcC*. **B:** *In vitro* kinase assay of ALK in neuroblastoma cells immunoprecipitated with αALK was performed as previously described.[27] Kinase reaction was performed without (**top panel**) or with (**bottom panel**) poly-Glu/Tyr (4:1) as exogenous substrates. Autophosphorylated ALK protein is marked by an **arrow**. Phosphorylated poly-Glu/Tyr is detected as smear indicated by the bracket. **C:** The expression patterns of other receptor tyrosine kinases in neuroblastoma cell lines. Each cell line was harvested, and about 30 μg of whole-cell lysates was subjected to Western blot analysis using the antibodies as indicated on the right. RET proteins are marked by **arrows**.

other types of solid tumor cell lines used as controls. *In vitro* kinase assay revealed outstanding ALK kinase activity in these three cell lines compared with other cells (Figure 1B), which is consistent with our previous study.[27] To examine whether overexpressed and activated ALK affects the expression of other RTKs in these cells, protein expression levels of RTKs, including EGFR, Ret, and TrkA, are compared with other cell lines. Significantly high levels of expression of EGFR and TrkA were observed in two of three cell lines overexpressing ALK (Figure 1C, top and bottom). Ret expression was commonly elevated in all three cell lines with activated ALK, especially in Nagai and NB-39-nu (Figure 1C, middle), consistent with previous study by Northern blotting.[32] Although it is unknown whether overexpression of these RTKs is related to overexpression of ALK, no obvious down-regulation of other RTKs was found in these *ALK*-amplified cell lines.

Inhibition of Activated ShcC, MAPKs, and Akt by Suppressing Activated ALK

To investigate the effect of suppressing the ALK expression level in *ALK*-amplified neuroblastoma cells using the RNAi technique, we synthesized two different RNA duplexes directed against nucleotide positions 153 to 171 and 399 to 417 within coding region *ALK* cDNA (ALK-siRNA1 and ALK-siRNA2, respectively). Because cotransfection of ALK-siRNA1 and ALK-siRNA2 was very effective in suppressing ALK expression, we performed all experiments presented here using a combination of two siRNAs, although similar results were obtained using only ALK-siRNA2. A sequence against the firefly luciferase gene (luc-siRNA) was used as a negative control. The expression of ALK protein is remarkably elevated in NB-39-nu and Nagai compared with other neuroblastoma cell lines, such as SK-M-MC (Figure 2A), caused by gene amplification.[27] The RNA duplexes were transfected into NB-39-nu cells with *ALK* gene amplification and SK-N-MC cells containing only a single copy of the *ALK* gene. We also tried to introduce ALK-siRNAs in several different neuroblastoma cell lines with or without *ALK* amplification in addition to NB-39-nu and SK-N-MC cells, resulting in partial or no reduction of ALK expression presumably due to the unsuccessful introduction in those cells. Therefore, we decided to use these two cell lines to perform further analysis of the effect of ALK knockdown by RNAi technique. RT-PCR analysis revealed that ALK mRNA level was reduced in both NB-39-nu cells and SK-N-MC cells treated with ALK-siRNAs, not in the cells treated with luc-siRNA and s-siRNA (Figure 2B). Both expression and phosphorylation of ALK kinase were significantly suppressed in the NB-39-nu cells treated with ALK-siRNAs compared with a mock-transfection control or cells treated with luc-siRNA (Figure 2C). In these cells, phosphorylation of ShcC was also suppressed despite the unchanged total amount of ShcC (Figure 2C), demonstrating that ShcC is a potent substrate of activated ALK kinase and that activation of ALK is actually responsible for the hyperphosphorylation of ShcC in these cancer cells. While the expression of downstream molecules, such as p44/42 MAPKs and Akt, was not affected by ALK-siRNAs, phosphorylation of these molecules was markedly reduced (Figure 2C). These results suggest that the Ras-MAPK pathway and the phosphatidylinositol 3-kinase/Akt pathway are dominantly regulated by activated ALK kinase in these cells. Interestingly, in SK-N-MC cells treated with ALK-siRNAs, phosphorylation levels of ShcC, p44/42 MAPKs, and Akt were not affected by

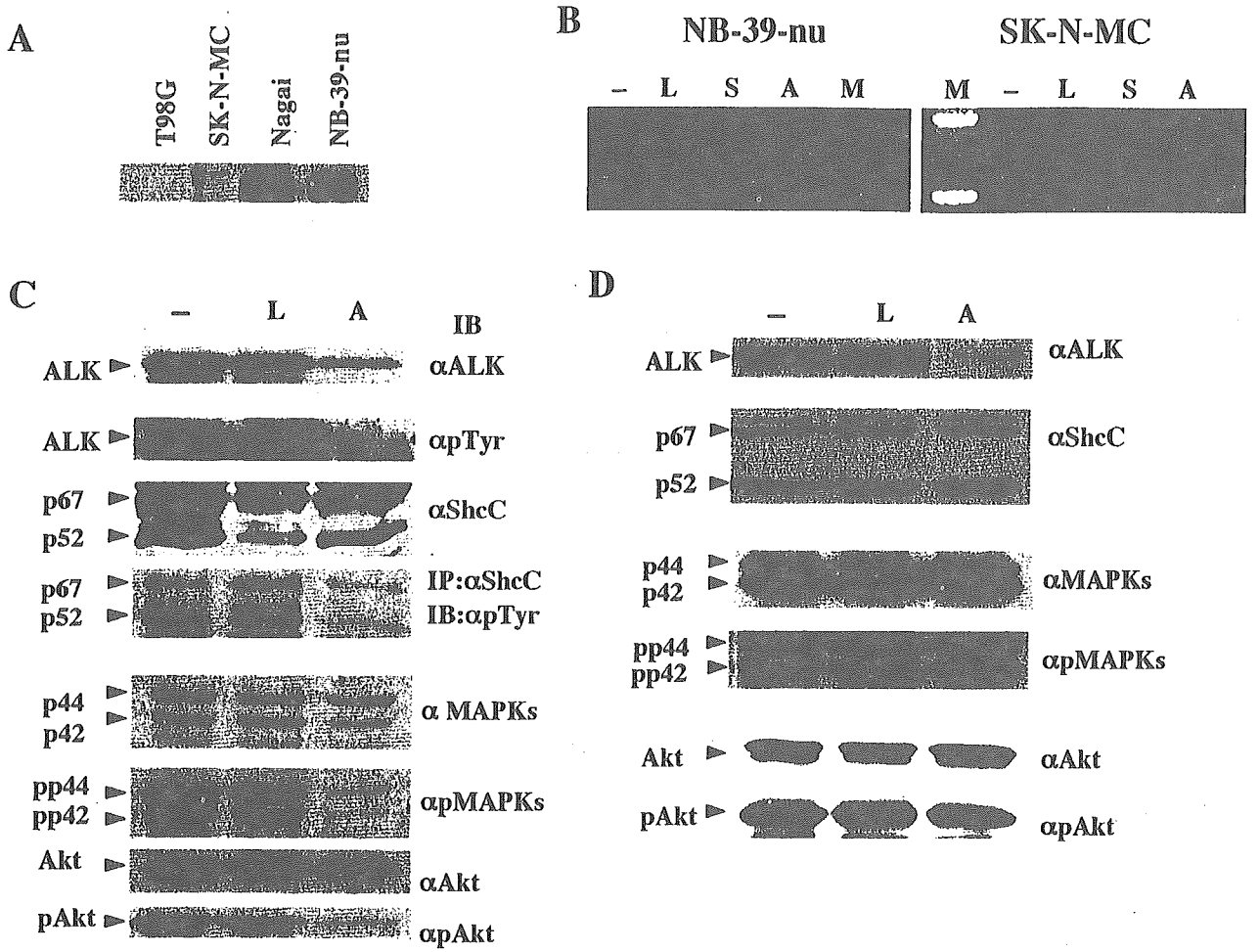

Figure 2. Suppression of ALK expression by siRNAs and changes in downstream molecules NB-39-nu cells and SK-N-MC cells. **A:** Expression levels of ALK protein in neuroblastoma cell lines including NB-39-nu and SK-N-MC. Each cell line was harvested, and about 30 μg of whole-cell lysates was subjected to Western blot analysis using αALK. **B:** mRNA levels of *Alk* in NB-39-nu cells. The cells were lysed at 84 hours after transfection and analyzed by RT-PCR. –, mock transfection; L, cells treated with luc-siRNA; S, cells treated with s-siRNA; A, cells treated with ALK-siRNAs; M, marker. **C:** NB-39-nu cells were harvested 84 hours after transfection. About 10 μg of whole-cell lysates or 250 μg of lysates immunoprecipitated with αShcC was subjected to Western blot analysis using the antibodies as indicated on the right. –, mock transfection; L, cells treated with luc-siRNA; A, cells treated with ALK-siRNAs. **D:** SK-N-MC cells were harvested 48 hours after transfection. About 10 μg of whole-cell lysates was subjected to Western blot analysis using the antibodies as indicated on the right. Bands of ShcC are marked by **arrows**. –, mock transfection; L, cells treated with luc-siRNA; A, cells treated with ALK-siRNAs.

ALK-siRNAs despite further suppression of the basal ALK expression level (Figure 2D), indicating that these pathways are not under the control of ALK in SK-N-MC cells.

Induction of Apoptosis by Suppression of Activated ALK

At 84 hours after transfection, apoptotic morphological changes, such as cell rounding, cytoplasmic blebbing, and irregularities of shape, were observed in NB-39-nu cells treated with ALK-siRNAs, whereas no significant changes were seen in the mock-transfected cells or in the luc-siRNA and the s-siRNA treated cells (Figure 3A). These morphological changes were not observed in SK-N-MC cells treated with ALK-siRNAs (data not shown). At 90 hours after transfection, NB-39-nu cells treated with ALK-siRNAs started to detach from the dish due to cell death.

To examine the localization of expression of ALK kinase, we performed double staining by anti-ALK antibody and TOTO-3, which stains the nucleus, in several neuroblastic cell lines. As shown in Figure 1D, unexpectedly, ALK protein overexpressed in NB-39-nu cells is localized in both membrane and cytoplasm. ALK staining was very weak in cell lines such as YT-nu and SK-N-MC with one copy of the *ALK* gene, however, its localization appeared to be the same as in NB-39-nu (data not shown). It was observed that the expression of ALK was completely lost after the RNAi-induced suppression of ALK (Figure 3C, top). To confirm whether the cell death resulted from apoptosis, cells were also analyzed by immunofluorescent TUNEL staining in NB-39-nu cells. TUNEL staining was clearly positive in these cells at 84 hours after transfection (Figure 3C, middle), indicating that apoptosis was induced in NB-39-nu cells treated with ALK-siRNAs. No significant TUNEL staining was observed in the mock-transfected cells or the luc-siRNA treated cells. Finally, DNA fragmentation assay was performed to measure the endonuclease activity accompa-

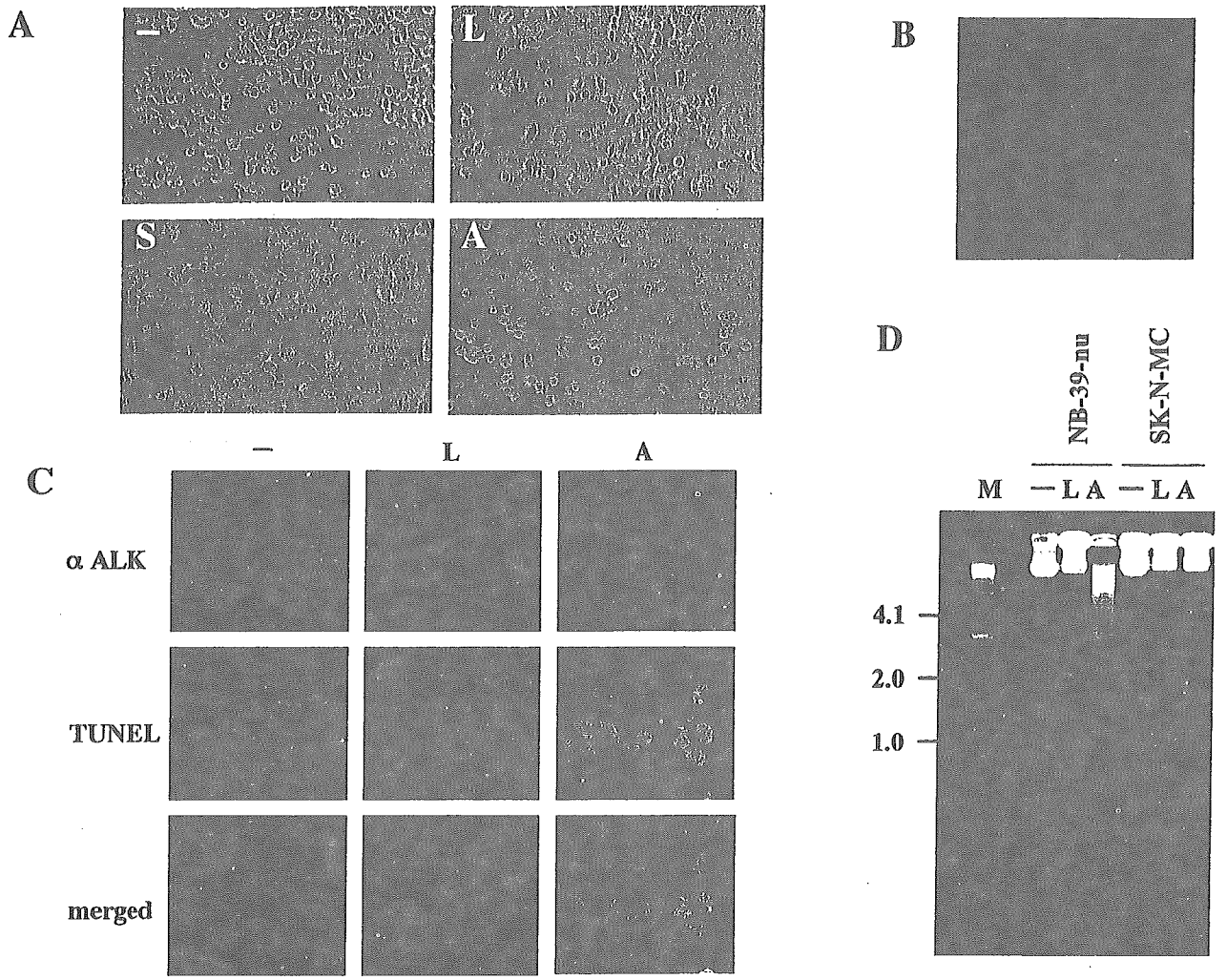

Figure 3. Induction of apoptosis in NB-39-nu cells treated with ALK-siRNAs. **A:** NB-39-nu cells on the dish were observed 84 hours after transfection under a light microscope. –, mock transfection; L, cells treated with luc-siRNA; S, cells treated with s-siRNA; A, cells treated with ALK-siRNAs. **B:** Cytoplasmic expression of ALK by immunocytostaining. The cells were stained for the expression of ALK (red) and apoptotic cells by TOTO-3 (blue). **C:** Cells on 24-well plates were fixed, and TUNEL assay was followed by staining with αALK (GST). The cells were stained for the expression of ALK (red) and apoptotic cells by TUNEL (green). –, mock transfection; L, cells treated with luc-siRNA; A, cells treated with ALK-siRNAs. **D:** DNA fragmentation assay in NB-39-nu cells and SK-N-MC cells treated with siRNAs. Genomic DNA was extracted 84 hours and 48 hours after transfection in NB-39-nu and in SK-N-MC, respectively. They were analyzed using electrophoresis. –, mock transfection; L, cells treated with luc-siRNA; A, cells treated with ALK-siRNAs; M, marker.

nied by apoptosis. The formation of significant DNA fragmentation was observed in the NB-39-nu cells but not in SK-N-MC cells treated with ALK-siRNAs (Figure 3D), indicating that cell apoptosis was induced through the suppression of ALK only in the NB-39-nu cells. This suggests that signaling pathways downstream of activated ALK dominantly regulate the survival of neuroblastoma cells with amplified ALK; therefore, the loss of ALK protein results in apoptotic changes to these cells.

Expression of ALK in Primary Neuroblastoma Tissues

Immunohistochemically, ALK was positively detected both in the cytoplasm of the neuroblastic cells and in the fine meshwork of neuropil of seven of nine tumors with favorable histology cases with nonamplified *N-myc* (FH&NA) (Figure 4, B and C). All seven unfavorable histology tumors (two UH&A tumors and five UH&NA tumors) were positive in the cytoplasm and/or in the fine meshwork of neuropil for ALK (Figure 4A). There was no correlation between the frequency or intensity of ALK-staining and histology of neuroblastoma tissues, showing majority of neuroblastoma samples showed a detectable amount of ALK. There was no significant staining using preimmune serum from the same rabbit as that for anti-ALK antibody (data not shown). Essentially the same results were obtained using a mouse monoclonal antibody against human ALK (ALK1: DAKO) (data not shown).

Amplification of the ALK Gene in Primary Neuroblastoma Tissues

It is essential to show whether ALK overexpression or gene amplification occurs in actual human neuroblastoma tissues in addition to neuroblastoma cell lines.

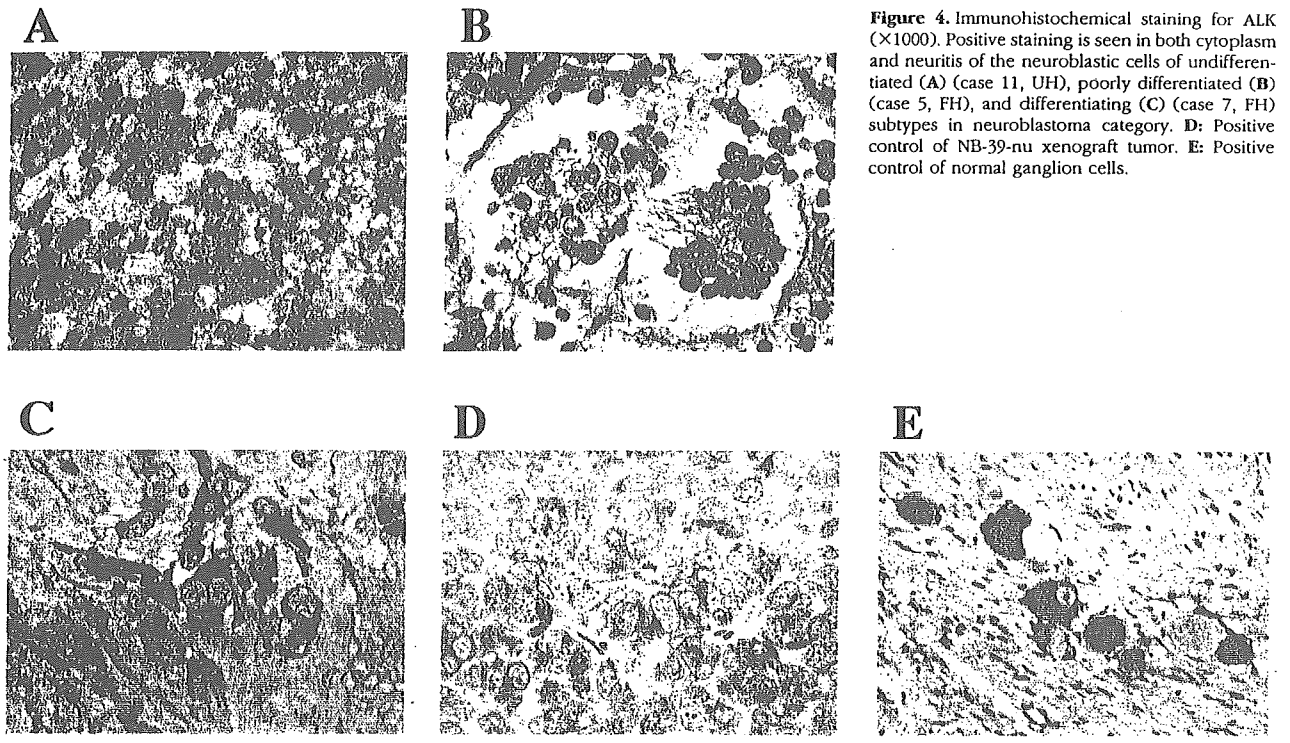

Figure 4. Immunohistochemical staining for ALK (×1000). Positive staining is seen in both cytoplasm and neuritis of the neuroblastic cells of undifferentiated (**A**) (case 11, UH), poorly differentiated (**B**) (case 5, FH), and differentiating (**C**) (case 7, FH) subtypes in neuroblastoma category. **D:** Positive control of NB-39-nu xenograft tumor. **E:** Positive control of normal ganglion cells.

Therefore, the mRNA amount of ALK kinase was first examined by RT-PCR on 32 primary neuroblastoma tissues (16 tissues with N-*myc* amplification and 16 tissues without N-*myc* amplification). Two of 32 cases showed slight elevation of *ALK* mRNA expression using several primer sets beyond the average expression level (data not shown).

To obtain more precise information about the copy numbers of *ALK*, we next analyzed the genomic DNAs of primary neuroblastoma tissues using Southern blot analysis. Whole purified DNA samples of tumors from 85 patients were examined. About the same number of N-*myc*-positive and N-*myc*-negative samples were collected to examine the relation between *Alk* and N-*myc* amplification. The intensities of signals on Southern blot membranes corresponding to the *ALK* gene and control *ShcC* gene, which is located on 9q22, were measured using a Molecular Imager FxPro (Bio-Rad), and the ratio of *ALK* signals to *ShcC* signals was calculated for each sample. Because more than 80% (70 samples) showed consistent ratios with each other in each experiment, these samples are treated as putative "single copy" controls. As several other samples showed apparently elevated intensity ratios, suggesting *ALK* amplification, relative copy numbers of *ALK* were calculated in comparison with average intensity ratios of putative single copy controls in each experiment. The results showed that there was significant *ALK* gene amplification in 8 of 85 patients (9.4%) (Figure 5). Seven of these eight cases, however, had only 1.8 to 3.0 copies of the *ALK* gene, suggesting a moderate gain of chromosomal focus rather than severe amplification. There was only one case that had outstanding amplification of ALK with approximately 10 copies. N-*myc* gene amplification was also detected in this case. The characteristics of the eight patients with *ALK* gain or amplification are shown in Table 1. Whereas seven of eight patients were classified as Stage III or IV (one as Stage III and six as Stage IV), the rest was classified as Stage I. The case with *ALK* amplification had N-*myc* amplification and was classified as Stage IV. Seven of eight patients were more than 1 year of age.

Discussion

Studies on ALK kinase demonstrate that activated ALK is involved in malignant tumor formation as forms of fusion proteins that force oligomerization of this kinase. We recently showed that the intact form of ALK protein is con-

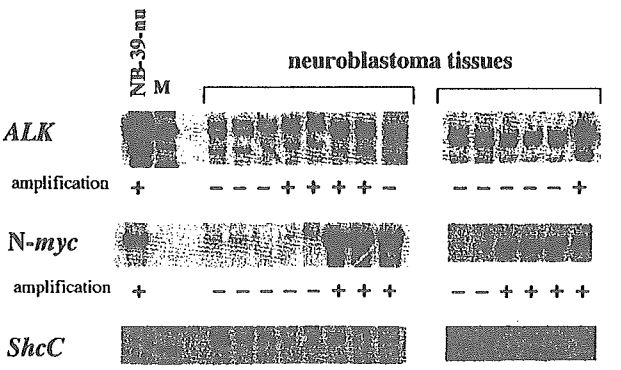

Figure 5. Detection of gene amplification of *ALK* and N-*myc* in primary neuroblastoma tissues. *ALK* was amplified in eight cases, and five of these eight cases are shown. The probe for *ALK* was removed from the filters, and the filters were re-hybridized in turn with other probes. Of eight cases with *ALK* amplification, N-*myc* amplification was detected in six cases and not detected in two cases. The probe for *ShcC* was used as a control for the amounts of DNA. M, marker.